



A simplified approach to satellite-based monitoring system of sugarcane plantation to manage yield decline at Wonji-Shoa Sugar Estate, central Ethiopia

Alemayehu Dengia^{a,*}, Nigussae Dechassa^b, Lemma Wogi^c, Berhanu Amsalu^d

^a Ethiopian Sugar Industry Group, Research and Training, P. O. Box,15, Wonji, Adama, Ethiopia

^b Haramaya University, College of Agriculture and Environmental Sciences, Africa Center of Excellence for Climate Smart Agriculture and Biodiversity Conservation, P. O. Box 138, Dire Dawa, Ethiopia

^c Haramaya University, School of Natural Resources Management and Environmental Sciences, P. O. Box 138, Dire Dawa, Ethiopia

^d Ethiopian Institute of Agricultural Research (EIAR), Melkassa Agricultural Research Centre, P.O. Box 436, Adama, Ethiopia

ARTICLE INFO

Keywords:

Canopy cover
Correlation
Landviewer
Platform
Sigmoid curve
Vegetation indexes
Yield components

ABSTRACT

Drastic and continuous decline in cane yields has become a major threat to sustainable sugarcane production in Ethiopia. Among the causes for the decline are the inefficient and ineffective system of monitoring sugarcane plantations. Adopting satellite-based crop monitoring through the Landviewer platform may circumvent this problem. However, the reliability of vegetation indexes calculated by the platform is unknown and thus requires evaluation. Accordingly, we tested the accuracy of selected Landviewer Calculated Vegetation Indexes (LCVIs) on three major sugarcane varieties and two cropping types. The goodness-of-fit of the sigmoid curve to the LCVIs profile of sugarcane was evaluated. The correlations between LCVIs and yield components, LCVIs and fractional green canopy cover (FGCC), as well as the time-series Normalized Difference Vegetation Index (NDVI) and yields, were also analysed. We found that the goodness-of-fit of the sigmoid curve was significant ($p < 0.001$), with 84%–95% accuracy in all the indexes. The majority of LCVIs showed significant ($p < 0.05$) relationships with yield components and FGCC. The time-series NDVI also demonstrated a significant relationship with cane yield ($R^2 = 0.73$ – 0.85) at the age of 10 months and above. The accuracy level of LCVIs varies with varieties and crop types, but the Normalized Difference Phenology Index (NDPI), Soil Adjusted Vegetation Index (SAVI), and NDVI were identified as the most consistent and effective LCVIs for sugarcane monitoring. Therefore, the accuracy of LCVIs was dependable and can be used effectively in monitoring sugarcane plantations to tackle the problem of continuous decline in the yield of the crop.

1. Introduction

Among the three other most productive crops in the world, namely, rice, wheat, and maize, sugarcane ranks first in crop tonnage and fourth in plant calories of the human diet [1]. Currently, about 26.5 million hectares of sugarcane are grown in 105 countries, with a total production of around 1.745 billion tons [2]. Brazil and India are the world's major producers of sugarcane, with annual outputs of approximately 769 million and 348 million metric tons, respectively [3,4]. African countries produce only 5% of the total global

* Corresponding author.

E-mail address: alex dengia@yahoo.com (A. Dengia).

<https://doi.org/10.1016/j.heliyon.2023.e18982>

Received 14 August 2022; Received in revised form 28 July 2023; Accepted 3 August 2023

Available online 5 August 2023

2405-8440/© 2023 The Authors. Published by Elsevier Ltd. This is an open access article under the CC BY-NC-ND license (<http://creativecommons.org/licenses/by-nc-nd/4.0/>).

sugar production, of which 80% is contributed by sub-Saharan African countries [4,5]. The leading sugarcane-producing countries in Africa are South Africa, Sudan, Swaziland, Zambia, Mauritius, and Kenya, accounting for more than 50% of the total production in the continent.

In Ethiopia, commercial sugarcane production started in 1951, during which a concession of 5000 ha of land was granted to the Dutch company United N.V. Handles Vereeniging Amsterdam (HVA) [6]. Considering the vast potential of the country [7–10], the Ethiopian government has made a large-scale investment since 2010 to expand the existing sugarcane plantations and establish new ones. Accordingly, it was planned to develop 400,000 ha of new sugarcane plantations [11], of which 102,000 ha have already been realized [12]. Upon accomplishing the plan, the sugar industry is expected to play a significant role in reducing poverty and ensuring the country's food security.

Despite such efforts, the continuous decline in yields of sugarcane has posed a severe threat to sustainable production of the crop in the country [13–15]. For instance, the cane yield at the Wonji-Shoa Sugarcane Plantation (WSSP) has declined by 48% over the last 70 years [15]. Thus, tackling the problem of such a continuous yield decline is a timely strategic issue of significance for the country.

One of the possible causes of the decline in sugarcane yield is the use of conventional methods of plantation monitoring. Such methods are inefficient and ineffective for sugarcane monitoring due to the canopy structure of the plant, which makes plantation fields extremely dense and difficult to navigate through, as well as the dangers posed to humans by various beasts and vermin inhabiting plantation fields, such as poisonous snakes, scorpions, spiders, etc. [16,17]. For instance, the number of corneal injuries caused by sugarcane leaves in India is 37% compared to wheat leaves, which is only 10.6% [17]. These situations prompted the International Labour Office (ILO) [18] to issue major 'Safety and Health Hazards' in accidents related to sugarcane field monitoring and management. Moreover, the hostile environmental conditions and the remote areas where the crop is often grown make the monitoring activity perilous, costly, and time-consuming [19,20]. As a result, it is difficult to timely detect and address the problems caused by various abiotic and biotic stresses on sugarcane plant.

To overcome these problems, alternative mechanisms for monitoring and detecting crop stress should be envisaged. In this regard, satellite-based crop monitoring offers the best opportunity since it enables plantation personnel to safely, effectively, and efficiently monitor crop health [21] and thus facilitates early intervention and management of potential problems before they spread widely [22]. As stated by Polivova and Brook [23], crop stresses detected in advance permit rapid adjustments in cropping system calendars and thus prevent yield penalties that may occur.

The benefit of satellite-based crop monitoring is being practically reaped in developed countries [22,24,25], whereas it has not yet been exploited in African countries [25,26]. Although a few studies have been conducted thus far in Ethiopia, the implementation of

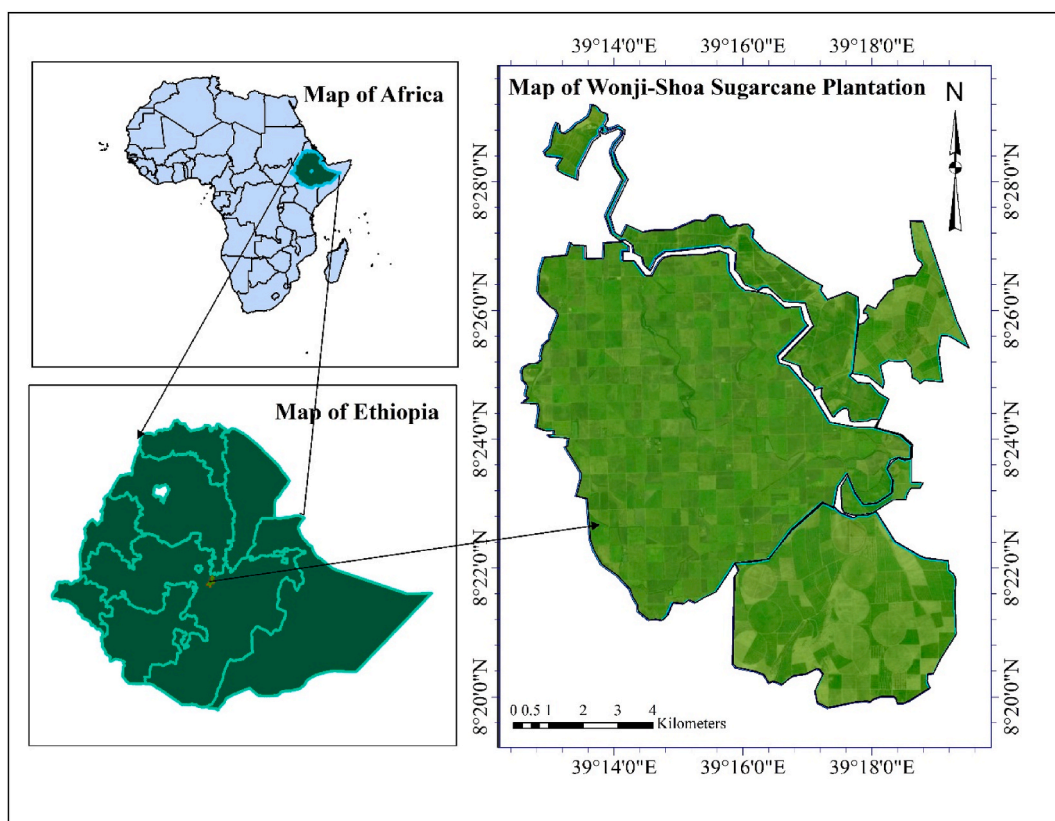


Fig. 1. Map of the study area.

the satellite-based crop monitoring system is negligible due to several constraints. For instance, the model developed on satellite-based estimation of yield for WSSP [27] could not be practically implemented by plantation personnel. This is because remote sensing data are big data and therefore require extensive computing capabilities and advanced skills [28], which cannot be found in African countries due to lack of resources and strategic frameworks [26,29].

Recently, a company named EOS-Data Analytics (<https://eos.com>) developed a simple and user-friendly satellite platform called Landviewer. Landviewer is a tool that analyses earth images and real-time observations via a browser [30]. Unlike conventional methods, Landviewer does not require downloading, processing and analysing an image manually [31]. Instead, it can directly search, process, and retrieve valuable insights from satellite images on the fly. All the images are stored and analysed on the Amazon cloud platform [30], and hence, operating the software does not require special skills and facilities. Therefore, this is an excellent opportunity for developing countries such as Ethiopia to leverage the vast potential of satellite-based crop monitoring and management systems. However, there have been no prior scientific studies conducted on the reliability of spectral vegetation indexes calculated by the Landviewer platform in the country.

Therefore, evaluating the relationship between ground truth data and different spectral vegetation indexes calculated by this platform is of paramount importance for exploiting the potential of satellite-based crop monitoring, which can make a significant contribution to alleviating the problem of declining yields of sugarcane in Ethiopia. As such, we aimed to evaluate selected vegetation indexes calculated by the Landviewer platform for monitoring sugarcane plantations and identify the most effective indexes in the central part of the country. Thus, we hypothesized that LCVIs are directly correlated with the sigmoid growth curve, yield components, Fractional Green Canopy Cover (FGCC), and final yield of sugarcane and enable us to monitor the performance of sugarcane plantations.

2. Material and methods

2.1. Description of study site

The study was conducted during the cropping seasons of 2020/2021 and 2021/2022 at Wonji-Shoa Sugarcane Estate, which is also called the Wonji-Shoa Sugar Factory, central Ethiopia. The site is located between 8°19'54"N–8°27'15"N and 39°12'34"E–39°19'21"E in Oromia Regional State, Adama District, 110 km southeast of Addis Ababa (Fig. 1). The altitude of the site ranges from 1540 to 1650 m above sea level, and the rainfall distribution is bimodal with erratic pattern. The mean annual long-year (1981–2021) rainfall is about 767 mm. Furthermore, the mean minimum and maximum temperatures are 14.7 °C and 27.4 °C, respectively, which are suitable for sugarcane production. The topography of the site is fairly flat and uniform (slope ranging from 0.02 to 0.05%) [13]. The Awash River, the sole perennial river in the Awash Basin, crosses the plain, dividing the plantation into west and east banks.

The Wonji-Shoa Sugar Estate was established in 1951 as a result of an agreement signed between the Dutch Company (H.V. Amsterdam) and the Ethiopian government. In 1954, the Wonji Sugar Factory launched sugar production, ushering an era of domestic sugar manufacturing in the history of Ethiopia. Currently, the sugarcane plantation covers around 11000 ha [12]. Wonji has an estimated population of 100000, of which 10678 are employees of the Sugar Factory [32,33].

The geology of the WSSP is a product of volcanic activity and rift tectonics, as it is located in Ethiopia's main rift valley region. Basalts, silicics, tuffs, ash flows, trachytes, and other volcanic rocks dominate the site's geological units. The age of the lacustrine rift material is congruent with the age of the Wonji volcanics, which mostly consist of volcano-clastic deposits and tuffs with silts, clays, and diatomites. Alluvial deposits are also widespread in some areas of the plantation [13].

According to the FAO soil classification, the major soil types in the WSSP area include Fluvisols, Andosols, and Leptosols [34], which are composed of a complex of grey cracking clays and semiarid brown soils in topographic depressions. They are classified as 'light' (coarse textured) or 'heavy' (clayey black kinds) based on texture [35]. The African Soil Atlas [36] spatial distribution reveals

Table 1

Morphological descriptions of the major sugarcane varieties grown at Wonji-Shoa Sugarcane Plantation.

SN	Characters	N14	NCo334	B52298
1	Leaf carriage	Erect	Semi-drooping	Erect
2	Leaf sheath spines	Dense	Glabrous	Sparse
3	Leaf sheath clasping	Tight	Tight	Tight
4	Leaf colour	Dark green	Green	Green
5	Ligule shape at Crescent	Crescent	Crescent	Crescent
6	Auricle shape at leaf sheath margin	Deltoid	Deltoid and sloppy	Deltoid
7	Lodging resistance	Tolerant	Moderately tolerant	Tolerant
8	Growth ring colour	Light green	Dull green	Light green
9	Leaf blade length (cm) (Fully expanded green leaf)	188	173	192
10	Leaf width (at the widest portion of the lamina) (cm)	4.47	4.32	5.58
11	Leaf colour	Dark Green	Green	Green
12	Leaf sheath colour	Green	Green	Green
13	Leaf sheath spines	Present	Absent	Present
14	Leaf sheath waxiness	Medium	Light	Light
15	Dewlap colour	Dull green	Green	Green

Source: Khan et al. [38].

that Silandic Andosols (clayey black types) are the prevalent soil in WSSP.

In WSSP, three major sugarcane varieties that cover 71% of the plantation have been grown: N14 (39%), NCo334 (20%), and B52298 (12%) [37]. Twenty minor varieties make up the remaining 29% of the plantation. The morphological descriptions of the varieties are illustrated in Table 1.

2.2. Satellite data

This study used the Sentinel-2 multispectral instrument (Sentinel-2) satellite since it has the best spatial (10–60 m) and temporal (5 days) resolutions of the freely available satellites. Furthermore, this satellite has 13 spectral bands (Table 2), including the red edge band, which is essential to detect the chlorophyll content of plants [28].

As part of the European Copernicus Programme, Sentinel-2 carries out a number of Earth observation missions, including agricultural monitoring [28]. It is a constellation of two twin satellites (Sentinel-2A and Sentinel-2B, which started operation in 2015 and 2017, respectively) and carries all multispectral instruments and acquires optical imagery from all over the globe. In this study, we used Sentinel-2A [39] since the average channel reflectance of Sentinel-2A MSI is greater than that of Sentinel-2B MSI over most channels [40].

Although the Sentinel-2 satellite enables more frequent and high-resolution observations of agricultural fields, it has been affected by cloud cover [21]. Furthermore, the view angle of Sentinel-2 is $\pm 10.3^\circ$ from the nadir view when acquiring observations, resulting in non-Lambertian surface directional reflectance effects [41].

2.3. Landviewer platform

Landviewer, a digital satellite-driven tool, was developed by a California-based company called EOS Data Analytics (EOSDA). The service enables on-the-fly satellite data searching, visualization, and processing by utilizing the platform's 10+ indexes or adding an index of interest. The software provides free access to medium-resolution images obtained from 10 satellites and, as a result, functions as a catalogue of satellite imagery acquired from various sensors. Users can also buy high- and extremely high-resolution imagery, as well as search and download images of any area [42].

In Landviewer (Fig. 2), image processing is executed on-the-fly, and the results of the primary analysis are instantly visualized on the screen. Unlike the conventional method, selection of the required date, location and sensor type is very easy due to an intuitive interface [30]. To use the platform, online registration is a prerequisite. Once registered, users can access up to 10 images per day for free, with the option to subscribe if more images are required.

2.4. Vegetation indexes

Vegetation indexes (VIs) are spectral transformations greater than or equal to two bands that are intended to increase the contribution of vegetation features and enable valid spatial and temporal inter-comparisons of terrestrial photosynthetic activity and alterations of canopy structure [43]. They can be used to track seasonal, inter-annual, and long-term changes in vegetation structural, phenological, and biophysical aspects. In this study, ten VIs, which have been extensively used in studies of vegetation properties [42, 44,45] were selected. The description of each VI and their corresponding equations (where NIR is near infrared, while B, R, G, and RE are blue, red, green and red-edge band reflectance, respectively) are described below.

2.4.1. Enhanced normalized difference vegetation index (ENDVI)

To provide a more sensitive result, the ENDVI compares green and blue light in addition to NIR light. This isolates plant health

Table 2
Spectral bands for the Sentinel-2 sensors.

Band Number	Sentinel-2A		Sentinel-2B		Spatial resolution (m)
	Central wavelength (nm)	Bandwidth (nm)	Central wavelength (nm)	Bandwidth (nm)	
1	442.7	20	442.3	20	60
2	492.7	65	492.3	65	10
3	559.8	35	558.9	35	10
4	664.6	30	664.9	31	10
5	704.1	14	703.8	15	20
6	740.5	14	739.1	13	20
7	782.8	19	779.7	19	20
8	832.8	105	832.9	104	10
8a	864.7	21	864	21	20
9	945.1	19	943.2	20	60
10	1373.5	29	1376.9	29	60
11	1613.7	90	1610.4	94	20
12	2202.4	174	2185.7	184	20

Source: The European Space Agency (<https://sentinels.copernicus.eu/web/sentinel/>)

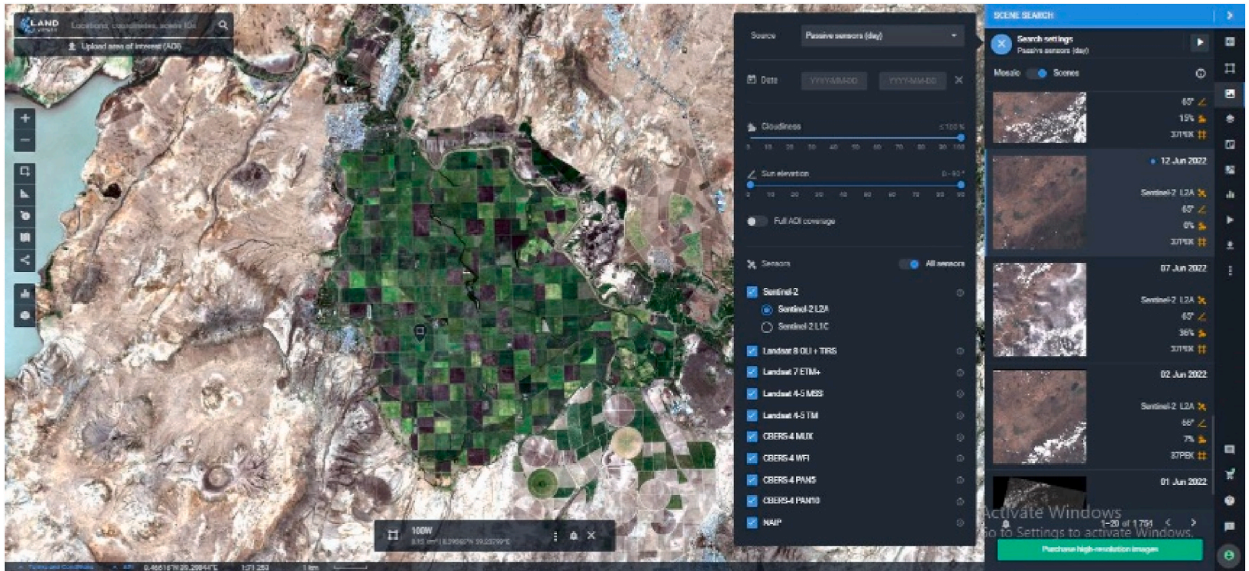


Fig. 2. Landviewer satellite platform depicting the natural colour of the Wonji-Shoa Sugarcane Plantation (<https://eos.com/landviewer/?lat=8.40912&lng=39.29612>).

indicators and can be used to determine the presence and health of a crop [46].

$$ENDVI = \frac{(NIR + G) - (2 * B)}{(NIR + G) + (2 * B)} \tag{1}$$

2.4.2. Green Differential Vegetation Index (GDVI)

GDVI take in to account near infrared (NIR) and green (G) bands to estimate nitrogen deficiency and requirements [47].

$$GDVI = NIR - G \tag{2}$$

2.4.3. Normalized Differential Vegetation Index (NDVI)

The NDVI is the most frequently used index to monitor drought, track and estimate crop yield, forecast hazardous fire zones, and map desert expansion. The NDVI is a standardized vegetation index that allows us to build an image of the relative biomass. The red (R) band chlorophyll absorption and the comparatively high reflectance of plants in the near infrared band (NIR) are used to calculate NDVI [45,48].

$$NDVI = \frac{NIR - R}{NIR + R} \tag{3}$$

2.4.4. The Soil-Adjusted Vegetation Index (SAVI)

The SAVI is a vegetation index that uses a soil luminance adjustment factor to reduce the influence of soil luminance. It is frequently utilized in desert settings where vegetation cover is minimal [43,45].

$$SAVI = \frac{1.5 * (NIR - R)}{NIR + R + 0.5} \tag{4}$$

2.4.5. The Enhanced Vegetation Index (EVI)

The EVI is an optimized vegetation index that is designed to improve vegetation monitoring by adding a blue band (B) with improved sensitivity in high biomass regions, a decoupling of the canopy background signal and a reduction in atmospheric influences [49].

$$EVI = \frac{2.5 * (NIR - R)}{(NIR + 6 * R - 7.5 * B) + 1} \tag{5}$$

2.4.6. Normalized Difference Phenology Index (NDPI)

The NDPI was developed to identify vegetation from soil and snow while minimizing discrepancies between these background components. On the other hand, the NDPI ignores the spectral features of dry grass. The NDPI employs the R, NIR, and shortwave infrared (SWIR) bands to differentiate vegetation from background components (soil and snow) [42,50].

$$NDPI = \frac{NIR - (0.74 * R + 0.26 * SWIR)}{NIR + (0.74 * R + 0.26 * SWIR)} \tag{6}$$

2.4.7. Normalized difference RedEdge (NDRE)

The NDRE is a photosynthesis activity indicator of vegetation cover that is used to measure nitrogen concentrations in plant leaves in the middle and end of a season. It is used to detect stressed and aging vegetation and to diagnose plant health by using NIR and RedEdge (RE) bands. It also makes it possible to optimize harvest timing and useful in the advanced ages of the crop. It is advisable to employ NDRE, where a dense canopy can produce NDVI saturation [45,51].

$$NDRE = \frac{NIR - RE}{NIR + RE} \tag{7}$$

2.4.8. Red-edge Chlorophyll Index (ReCI)

The ReCI is a photosynthetic activity index of vegetative cover that is sensitive to chlorophyll content in leaves. Because chlorophyll levels are closely tied to nitrogen levels in the crop, the index helps to identify parts of the field with yellowed or faded leaves that may require further fertilizer treatment [45,52].

$$RECI = \frac{NIR}{RE} - 1 \tag{8}$$

2.4.9. Ratio Vegetation Index (RVI)

The RVI has a high ability to indirectly signal chlorophyll and nitrogen content in leaves, leaf area, and dry weight and hence has a high potential to estimate insect pest damage to crops [53,54].

$$RVI = \frac{NIR}{R} \tag{9}$$

2.4.10. Green Normalized Difference Vegetation Index (GNDVI)

The GNDVI is a modified version of the NDVI that incorporates green (G) and near-infrared (NIR) light to better show chlorophyll content and changes in vegetation. It is also beneficial for analysing the crop’s water and nitrogen deficits and excesses [52].

$$GNDVI = \frac{NIR - G}{NIR + G} \tag{10}$$

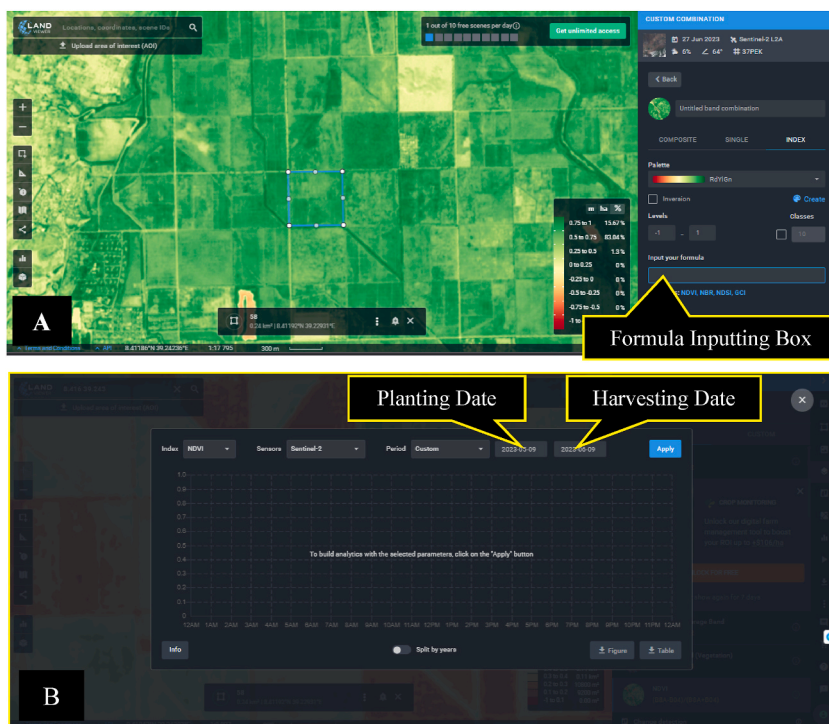


Fig. 3. A Landviewer platform showing the ‘Custom Combination’ feature that permits input of a new formula (A) and the ‘Time Serious Analyses’ feature that allows entering planting and harvesting dates (B) to generate time series NDVI values of an area of interest.

2.5. Evaluation approaches

The Landviewer platform allows users to calculate any spectral index by entering the formula into the custom combination tab (Fig. 3A). It also generates the time series NDVI value of any desired area of interest from planting to harvesting in the platform's time series tab (Fig. 3B). In this study, four approaches were utilized to compare the results derived from both features of the platform against ground data collected from the fields of WSSP.

2.5.1. Goodness-of-fit of the sigmoid growth curve in the LCVI profiles of sugarcane

The growth of the sugarcane plant follows a sigmoidal growth curve [16]. A sigmoid growth curve (S-shaped growth curve) is a type of growth in which a living organism increases in population, initially at a slow rate (lag phase), then at an exponential rate (log phase), and finally at a decreasing rate (stationary phase) until the population stabilizes [55].

Of the different types of sigmoid growth curves, the growth of a newly planted sugarcane field is better described by a logistic curve that defines symmetric growth, and the growth of the ratoon cane is better explained by the Gompertz model, which depicts asymmetric growth with fixed inflection points [56,57]. Thus, in our study, the plant and ratoon cane fields were evaluated separately by employing goodness-of-fit of the Logistic curve [58] and Gompertz curve [59], respectively, during the first 10 months of cane age.

2.5.2. Relationship between yield components and LCVIs

The second approach focused on evaluating LCVIs for their degree of association with yield components of sugarcane (plant density, height, and diameter). These yield components have a significant association with cane yield and hence can show the performance (health) of the cane [60]. Thus, spectral VIs are expected to correlate with these yield components.

2.5.3. Relationship between fractional green canopy cover (FGCC) and LCVIs

Fractional green canopy cover (FGCC) is an indicator of canopy development, light interception, and evapotranspiration partitioning, which are indicators of crop health [61]. Earlier studies in other crops indicate that spectral vegetation indexes, mainly NDVI, are significantly correlated with FGCC [62–64].

2.5.4. Relationships between sugarcane yield and time series NDVI

One of the ingenious features of Landviewer is that it can automatically generate the whole NDVI values during the entire growth period of the cane once the planting and harvesting date is specified [45]. This enables farm managers to easily assess the performance of a crop instantly. Thus, the relationship between Normalized Difference Vegetation Index (NDVI) and the final yield of sugarcane was evaluated.



Fig. 4. An example of the field layout of one of the sampled fields (variety NCo334) from which yield components of sugarcane were collected.

2.6. Field data collections

The fields selected for data collection had an area of 5–24 ha and were harvested during the cropping seasons of 2020–2021 and 2021–2022. The average harvest ages were 18 and 14 months for the plant and ratoon cane, respectively. The ratoon fields used for the study were selected from the first and second cuttings. In WSSP, the harvesting season lasts from November to May, while the peak planting months are December–March. Data and information that comprise the crop type, variety, average yield, planting/ratooning date, and harvesting date of each of the selected field were obtained from a historical yield database archived by Wonji-Shoa Sugar Factory.

- A. To test the goodness-of-fit of the sigmoid curves, a stratified sampling method was applied. Accordingly, the two crop types (plant crop and ratoon crop) were used as the main strata, and from each crop type, three varieties (NCo334, N14, and B52298) were used as substrata. Finally, three fields that were harvested in a cropping season of 2020–2021 with a reasonable yield (above 100 tons ha^{-1}) were randomly selected from each substrata. Then, the planting and harvest dates of each field were extracted from the database brought from Wonji-Shoa Sugar Factory.
- B. To collect data pertaining to the yield components of sugarcane, one ratoon field was selected randomly from each of the three major sugarcane varieties, i.e., NCo334, N14, and B52298, that were harvested in the 2020–2021 cropping season. When the cane reached the grand growth stage (6 months of age), approximately 5 ha of the selected fields were delineated and laid out into nine main plots, each with an area of 1392 m^2 (Fig. 4). The layout was created in such a way that the plots were uniformly distributed across the entire field. Then, the geo-references of each plot were recorded using a Global Navigation Satellite System (GNSS) receptor. To collect ground truth data, each plot was further divided into three subplots (46.4 m^2), and plant density, height, and diameter were collected and extrapolated for the main plot. The plant density was determined by counting the number of millable cane stalks within the subplots. Plant height (from ground level up to the top visible dewlap) and cane diameter (at the middle of the stalk) were measured by randomly selecting three cane stalks from each subplot.
- C. To determine the fractional green canopy cover (FGCC), stratified sampling, where the three major sugarcane varieties of WSSP were used as strata, was employed. From each stratum, three fields with an age of four to five months were selected randomly. Depending on the shape and area of each field, two to five plots of approximately 600–800 m^2 were demarcated on a randomly selected site. The geo-references of each plot were recorded using a GNSS receiver. Then, from each plot, three to four spots were randomly selected, and the top images of the cane canopy were taken from a height of about 3.5 m using a smartphone (Techno C9) mounted on a stick (Fig. 5). In total, 108 pictures were taken, and the FGCC was calculated by analysing the collected images using Canopeo software (Oklahoma State University, Stillwater, OK). The calculations were performed as per the guidelines indicated on the official website of the application (<https://canopeoapp.com/>). Canopeo is a tool of image analysis that gives a percentage of white pixels (Fig. 5), which corresponds to green canopy coverage [61]. The FGCC value obtained from each spot was then extrapolated into the main plot. The field data were collected on the same day as the imagery date of the study area by the Sentinel-2 satellite.
- D. To evaluate the time series NDVI values generated by Landviewer, ratoon sugarcane fields that recorded a yield of 24–140 ton ha^{-1} were randomly selected from the field-level database of the Wonji-Shoa Sugar Factory. From each of the three major varieties, N14, NCo334 and B52298, 29 fields were selected, making a total of 87 fields selected.

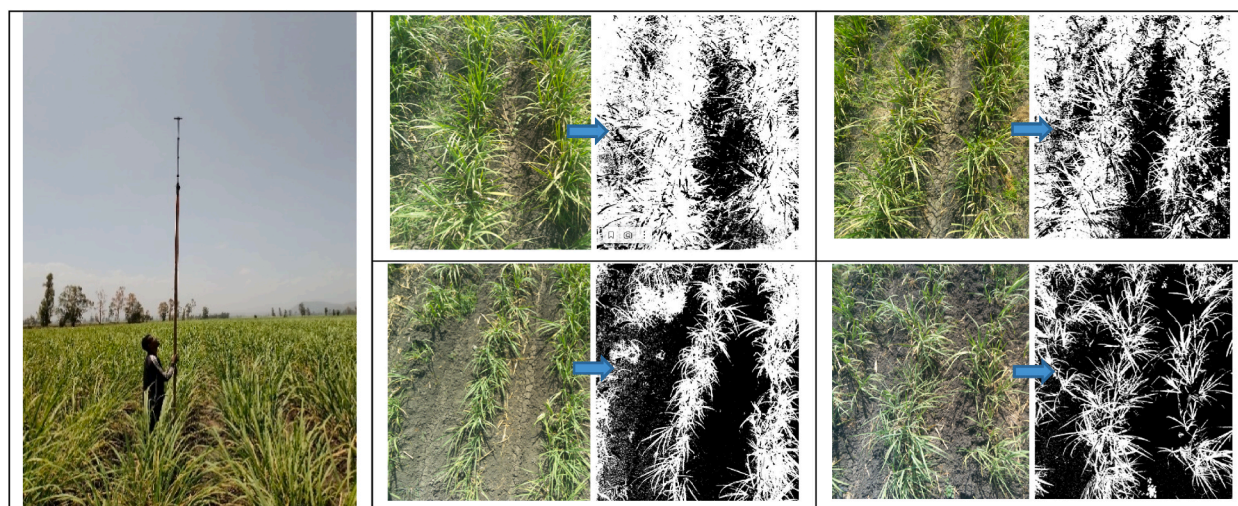


Fig. 5. Cane image as taken from a height of 3.5 m (left) and analysed by Canopeo (right). The percentage of the white pixels in the analysed images correspond to green canopy coverage.

To determine the vegetation index (VI), first, a polygon of each selected field/plot (areas of interest) was drawn on Google Earth Pro. When the entire field was used as an area of interest, a polygon was drawn by following the border of that specific field. Whereas, when a plot within a field was used as an area of interest, the coordinates collected from the corner of each plot were imported to Google Earth Pro, and then a polygon was drawn following these coordinates. Second, the polygons drawn on Google Earth Pro were saved as a kml file and uploaded to the Landviewer platform (Fig. 2). Third, the vegetation indexes were determined by inserting the formula for each index into the formula input field under the custom combination tab of the Lanviewer (Fig. 3A). Fourth, to determine the mean index value of an area of interest, the weighted mean of the mid-values of each performance category was calculated. Fifth, the time-series NDVI values were generated by entering the planting or ratooning dates as well as harvest dates of a field in the period box of the time-series analysis tab (Fig. 3B). Finally, the entire set of NDVI values (planting date/ratooning date to harvest date) was downloaded from the platform as an Excel file. A schematic representation of the whole methodology is depicted in Fig. 6.

2.7. Data analysis

Genstat 2018 [65] was used to test the significance of the goodness-of-fit of the sigmoid curve in LCVIs. Then, the percentage variance accounted for the goodness fit of logistic and Gamperz curves for plant and ratoon canes, respectively, was taken to compare the LCVIs. To that end, mean separation by using Tukey’s test at 95% confidence intervals was analysed.

To evaluate the significance and the degree of relationship between LCVIs vs. FGCC and LCVIs vs. yield components of sugarcane, a regression analysis was performed using real statistics resource pack software (Release 7.6) [66].

From the downloaded file of time-series NDVI values for each field, the mean of three maximum NDVI values [67] at 2, 4, 6, 8, and 10 months of age as well as at harvest were computed. Then, multiple linear regressions were carried out between the mean value of the NDVI and the final yield of the cane using the same software.

3. Results

3.1. Goodness-of-fit of sigmoid growth curve to Landviewer Calculated Vegetation Indexes (LCVIs)

For each sugarcane variety, the goodness-of-fits of the logistic and Gamperz curves of all the Landviewer Calculated Vegetation Indexes (LCVIs) were significant ($p < 0.001$) for both plant and ratoon crops, respectively (Fig. 7). The temporal profiles of LCVIs showed an initial gradual increase, followed by an exponential rise, and then becoming stagnant (Fig. 7). However, the trends observed

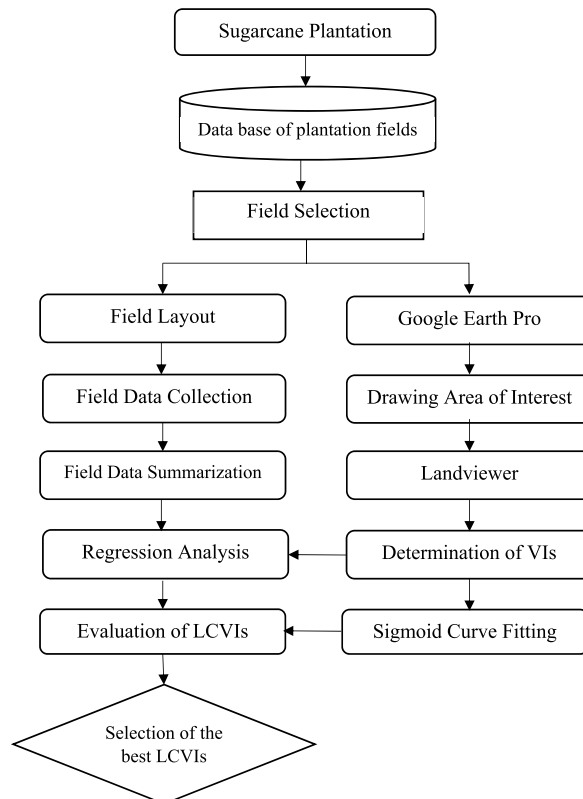


Fig. 6. Flow chart of the methodology. LCVIs and VIs stand for Land viewer Calculated Vegetation Indexes and Vegetation Indexes, respectively.

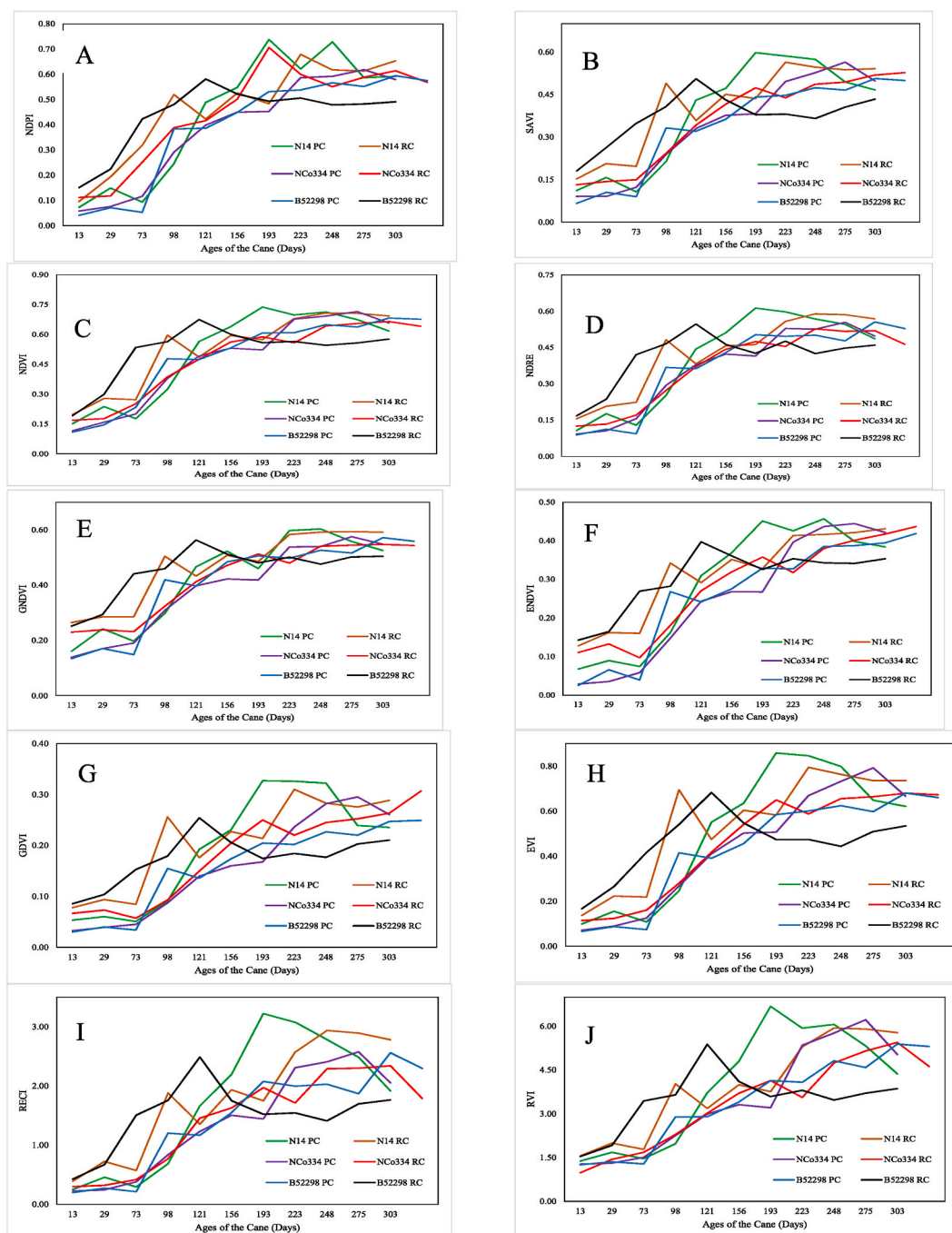


Fig. 7. Landviewer Calculated Vegetation Indexes (LCVIs) profile of sugarcane during the first 10 months age of the crop on the three major varieties (N14, NCo334 and B52298) and the two crop types (PC and RC, plant cane and ratoon cane, respectively) at Wonji-Shoa Sugarcane Plantations in central. Ethiopia. Each alphabet represents one of the ten VIs i.e. NDPI (A), SAVI (B), NDVI (C), NDRE (D), GNDVI (E), ENDVI (F), GDVI (G), EVI (H), RECI (I) and RVI (J). Each curve is an average of three fields and significantly fitted to sigmoid growth model at $p < 0.001$.

in the Normalized Difference Phenology Index (NDPI) (Fig. 7A), Soil Adjusted Vegetation Index (SAVI) (Fig. 7B), Normalized Difference Vegetation Index (NDVI) (Fig. 7C), Normalized Difference Red Edge (NDRE) (Fig. 7D), Green Normalized Difference Vegetation Index (GNDVI) (Fig. 7E), Enhanced Normalized Differential Vegetation Index (ENDVI) (Fig. 7F), Green Differential Vegetation Index (GDVI) (Fig. 7G), and Enhanced Vegetation Index (EVI) (Fig. 7H) were found to be better than those in the Red-edge Chlorophyll Index (ReCI) (Fig. 7I), and Ratio Vegetation Index (RVI) (Fig. 7J) in terms of following sigmoidal growth pattern. This was also in agreement with the results indicated in Table 3. Furthermore, the rate of increase at the early stage of growth was slower in the plant cane than in the ratoon cane, which may result from the fact that the latter had an already established root system.

An example used to illustrate temporal change in VIs (time series NDVI map of one of the sampled plant cane fields) also shows a pictorial representation of the aforementioned results where the differences among the NDVI of successive months were initially low (germination stage) (Fig. 8A and B) and then drastically increased until the cane reached 6 months of age (Fig. 8C, D, Fig. 8E, and Fig. 8F). Finally, the NDVI becomes stagnant at the grand growth phase (Fig. 8G, H, and Fig. 8I). This again confirmed that LCVIs follow the typical growth trend of the sugarcane crop, i.e., a sigmoidal growth pattern [16]. Hence, LCVIs can be used effectively to monitor the performance of sugarcane plantations and make decisions about the management of the crop during its growth stages.

Tukey’s test at the 95% confidence interval revealed the existence of significant differences among the LCVIs. Accordingly, the goodness-of-fit in SAVI, NDPI, NDRE, EVI, GNDVI, GDVI and ENDVI (91–95% of the variability) were significantly ($p < 0.05$) higher than RVI and RECI (80–89% of the variability) (Table 3), while there were no significant differences among the VIs within both the former and the latter groups (Table 3). Hence, except for the RVI and RECI, all the LCVIs can be used to monitor both plant and ratoon

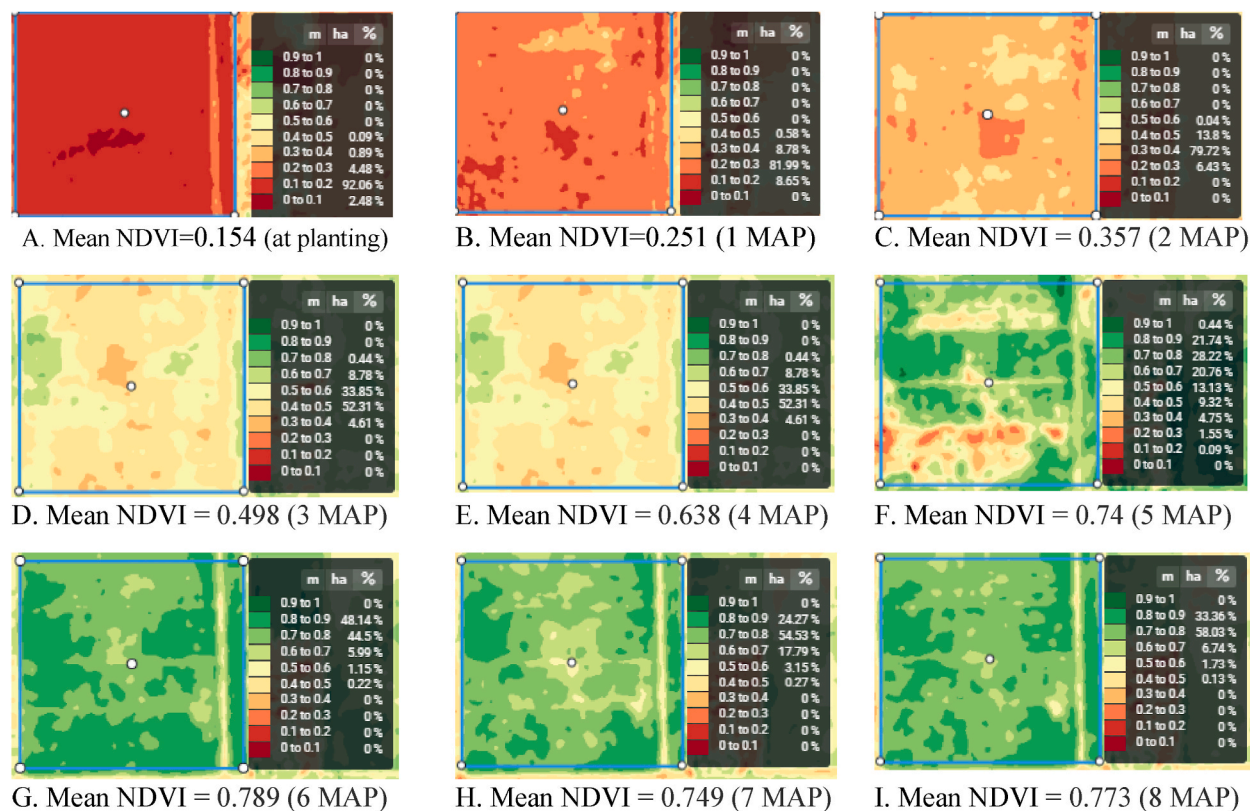


Fig. 8. An example of the vegetation index (NDVI) of a sugarcane field at different months after planting (MAP) showing that the growth of sugarcane follows a sigmoid growth pattern.

Table 3

Percent variance accounted for sigmoid growth curve fitting in Landviewer Calculated Vegetation Indexes (LCVIs) on the three major varieties (N14, NCo334 and B52298) and the two crop types (plant cane and ratoon cane) at Wonji-Shoa Sugarcane Plantation in central Ethiopia.

Index	Plant Crop				Ratoon Crop			
	NCo334	B52298	N14	Mean	NCo334	B52298	N14	Mean
SAVI	97.50	96.40	91.50	95.13a	95.50	90.53	93.07	93.03a
NDPI	97.10	95.00	93.07	95.06a	92.50	91.90	93.33	92.58a
NDRE	96.10	95.27	92.33	94.57 ab	94.07	92.83	90.23	92.38a
NDVI	96.13	94.93	92.53	94.53 ab	96.40	85.20	94.40	92.00a
EVI	97.90	95.27	88.80	93.99 ab	94.43	86.07	94.07	91.52a
GNDVI	96.07	95.67	89.37	93.70 ab	96.70	80.83	95.23	90.92 ab
GDVI	97.83	94.67	84.97	92.49abc	92.17	92.10	88.23	90.83 ab
ENDVI	96.97	91.67	85.27	91.30abc	95.07	84.97	91.60	90.54 ab
RVI	92.03	90.87	73.47	85.46bc	86.90	71.67	89.53	82.70bc
RECI	87.30	91.27	73.17	83.91c	87.63	72.00	82.10	80.58c
Mean	95.49a	94.10a	86.45b	92.01	93.14a	84.71b	91.18a	89.1

The goodness of fit was tested by fitting logistic and Gampertz growth curve to LCVIs in the plant and in the ratoon crops, respectively. The comparison was made by using Tukey’s test at 95% confidence intervals.

cane fields with better accuracy.

The performance of LCVIs in relation to sugarcane varieties showed significant differences. We found that the goodness-of-fit of the logistic curve for NCo334 (95% of variability) and B52298 (94% of variability) were in statistical parity, whereas the values of the goodness-of-fit of the logistic curve of both varieties were significantly higher than that of N14 (86% of variability) in the plant crop. In the case of the ratoon crop, NCo334 (93% of variability) and N14 (91% of variability), which were not significantly different, performed better than B52298 (85% of variability). This implies that the VIs to be used for monitoring different varieties may also vary. Table 3 indicates that the best indexes for the monitoring of the NCo334, B52298 and N14 varieties were EVI, SAVI, and NDPI, respectively, for plant cane fields. In the case of ratoon fields, GNDVI was found to be the best index for monitoring both NCO334 and N14, while NDRE was the most effective evaluator of B52298.

Compared to the plant crop, the LCVIs from ratoon cane showed inferior fittings in all the corresponding indexes (Table 3). The combined mean goodness-of-fit in ratoon cane (89% of variability) was also lower than that in plant cane (92% of variability). This implies that during monitoring of ratoon crops, the LCVIs to be used should be selected carefully (Table 3).

3.2. Relationship between yield components and Landviewer Calculated Vegetation Indexes (LCVIs)

3.2.1. Variety NCo334

All the LCVIs, except the Enhanced Normalized Difference Vegetation Index (ENDVI), showed significant ($p < 0.05$) relationships with plant density, plant diameter, and plant height (Table 4). Of the three yield components, we observed the strongest relationship in plant density ($R^2 = 0.66$ – 0.90), followed by plant height ($R^2 = 0.38$ – 0.70) and plant diameter ($R^2 = 0.35$ – 0.65).

When a combined regression analysis (using the three yield components as independent variables) was applied, all the LCVIs (except ENDVI) exhibited significant ($p < 0.05$) relationships with the yield components (Table 4). Among the indexes, the Green Difference Vegetation Index (GDVI), Green Normalized Difference Vegetation Index (GNDVI), Normalized Difference Vegetation Index (NDVI), and Soil Adjusted Vegetation Index (SAVI) ($R^2 > 0.90$) showed relatively stronger correlations than the Enhanced Vegetation Index (EVI), Red-edge Chlorophyll Index (RECI), Normalized Difference Phenology Index (NDPI), Normalized Difference Red Edge Index (NDRE), and Ratio Vegetation Index (RVI). In fact, the three yield components and the VIs were correlated with different degrees of accuracy. The plant density was better correlated with the GDVI ($R^2 = 0.9$), while both plant height ($R^2 = 0.74$) and diameter ($R^2 = 0.65$) showed a better correlation with the GNDVI. Hence, these indexes can be selected as the best tool to assess the yield components of sugarcane.

3.2.2. Variety N14

Except for ENDVI and NDVI, there existed a significant relationship between plant density and LCVIs, where SAVI and RVI ($R^2 = 0.64$) showed the highest degree of relationship (Table 5). In the case of plant height, the relationship was significant for all the LCVIs, with EVI ($R^2 = 0.88$) and SAVI ($R^2 = 0.88$) being the highest. In contrast to variety NCo334, the strongest relationship was observed in plant height, while no significant association was observed in stalk diameter, indicating that varieties have different reflectance properties.

Concerning the combined regression analysis, all the LCVIs showed a significant and strong relationship ($p < 0.05$) with the three variables in common (Table 5). The highest and lowest coefficients of determination were recorded for the NDPI, SAVI, RECI, and EVI ($R^2 = 0.89$ – 0.92), as well as for the GDVI and EDVI ($R^2 = 0.73$), respectively (Table 5).

3.2.3. Variety B52298

Unlike the aforementioned varieties, yield components of B52298 showed poor association with LCVIs, which suggests that monitoring this variety by using LCVIs needs special attention and that an alternative mechanism should be sought (Table 6). The plant density was significantly ($p < 0.05$) related to the GDVI ($R^2 = 0.66$), EVI ($R^2 = 0.64$), SAVI ($R^2 = 0.62$), NDPI ($R^2 = 0.60$), and NADRE ($R^2 = 0.60$) but was not significantly associated with the remaining indexes ($0.22 \leq R^2 \leq 0.5$) (Table 6). Plant height ($0 \leq R^2 \leq 0.18$) and plant diameter ($0 \leq R^2 \leq 0.23$) showed no significant and very weak correlations. In the combined regression analysis, except for

Table 4

The strength and significance of relationship between Landviewer Calculated Vegetation Indexes (LCVIs), and plant density, height and diameter in variety NCo334 at Wonji-Shoa Sugarcane Plantation in central Ethiopia.

Index	Plant density		Plant height		Plant diameter		Combined	
	R^2	p -value	R^2	p -value	R^2	p -value	R^2	p -value
NDPI	0.81	<0.001	0.66	0.01	0.61	0.01	0.86	0.01
GDVI	0.90	<0.001	0.71	<0.001	0.63	0.01	0.93	<0.001
ENDVI	0.66	0.01	0.38	0.08	0.35	0.09	0.70	0.05
SAVI	0.88	<0.001	0.54	0.02	0.50	0.03	0.91	<0.001
NDVI	0.88	<0.001	0.60	0.02	0.54	0.02	0.91	<0.001
NDRE	0.80	<0.001	0.64	0.01	0.64	0.01	0.86	0.01
RVI	0.74	<0.001	0.70	0.01	0.64	0.01	0.84	0.01
RECI	0.84	<0.001	0.70	0.01	0.61	0.01	0.87	<0.001
EVI	0.84	<0.001	0.60	0.01	0.56	0.02	0.88	<0.001
GNDVI	0.88	<0.001	0.74	<0.001	0.65	0.01	0.92	<0.001

Table 5

The strength and significance of relationship between Landviewer Calculated Vegetation Indexes (LCVIs), and plant density, height, and diameter in variety N14 at Wonji-Shoa Sugarcane Plantation in central Ethiopia.

Index	Plant density		Plant height		Plant diameter		Combined	
	R ²	p-value	R ²	p-value	R ²	p-value	R ²	p-value
NDPI	0.63	0.01	0.86	<0.001	0.13	0.33	0.92	<0.001
GDVI	0.56	0.02	0.70	0.01	0.01	0.85	0.73	0.04
ENDVI	0.41	0.06	0.73	<0.001	0.06	0.53	0.73	0.04
SAVI	0.64	0.01	0.88	<0.001	0.06	0.54	0.90	<0.001
NDVI	0.44	0.05	0.72	<0.001	0.03	0.66	0.72	0.04
NDRE	0.60	0.02	0.76	<0.001	0.05	0.57	0.79	0.02
RVI	0.64	0.01	0.67	0.01	0.00	0.87	0.75	0.03
RECI	0.60	0.01	0.87	<0.001	0.10	0.40	0.90	<0.001
EVI	0.60	0.02	0.88	<0.001	0.07	0.50	0.89	<0.001
GNDVI	0.52	0.03	0.74	<0.001	0.04	0.62	0.75	0.03

Table 6

The strength and significance of relationship between Landviewer Calculated Vegetation Indexes (LCVIs), and plant density, height and diameter in variety B52298 at Wonji-Shoa Sugarcane Plantation in central Ethiopia.

Index	Plant density		Plant height		Plant diameter		Combined	
	R ²	p-value	R ²	p-value	R ²	p-value	R ²	p-value
NDPI	0.60	0.02	0.17	0.31	0.23	0.23	0.77	0.05
GDVI	0.66	0.02	0.18	0.29	0.19	0.29	0.76	0.05
ENDVI	0.39	0.10	0.11	0.41	0.10	0.45	0.66	0.38
SAVI	0.62	0.02	0.05	0.58	0.08	0.51	0.73	0.07
NDVI	0.50	0.05	0.04	0.66	0.08	0.49	0.65	0.12
NDRE	0.60	0.02	0.05	0.61	0.07	0.54	0.69	0.09
RVI	0.50	0.05	0.04	0.63	0.11	0.42	0.69	0.09
RECI	0.22	0.24	0.00	0.92	0.00	0.93	0.33	0.54
EVI	0.64	0.02	0.08	0.49	0.14	0.37	0.79	0.04
GNDVI	0.50	0.05	0.03	0.67	0.06	0.56	0.61	0.17

EVI (R²-0.79), all the LCVIs were also not significant.

3.3. Fractional green canopy cover (FGCC)

A significant ($p < 0.05$) association was observed between LCVIs and FGCC in nine of the indexes for variety NCo334, in eight of the indexes for variety N14, and in four of the indexes for variety B52298 (Table 7). Hence, similar to the findings observed in the yield components (Tables 4–6), variety B52298 again demonstrated poor correlation with FGCC (Table 7).

In variety Nco334, the highest association was observed in SAVI (R² = 0.79), which was followed by RVI (R² = 0.74), NDVI (R² = 0.72), and NDPI (R² = 0.72). For N14, the highest association was also found in SAVI (R² = 0.93), followed by ENDVI (R² = 0.87), NDPI (R² = 0.83), and NDRE (R² = 0.74). For B52298, only NDVI (R² = 0.83), NDPI (R² = 0.73), NDRE (R² = 0.71), and GNDVI (R² = 0.67) showed a significant relationship with FGCC.

In general, the NDPI, NDVI, and GNDVI showed significant relationships with the FGCC for all the three varieties (Table 7), which again confirms the consistent performances of mainly the NDPI under different conditions. However, ENDVI, SAVI, NDRE, RVI, and

Table 7

The strength and significance of relationship between Landviewer Calculated Vegetation Indexes (LCVIs) and Fracrional Green Canopy Cover (FGCC) for the major sugarcane varieties at Wonji-Shoa Sugarcane Plantation in central Ethiopia.

Index	NCo334		N14		B52298	
	R ²	p-value	R ²	p-value	R ²	p-value
NDPI	0.72	<0.001	0.47	0.03	0.73	0.01
GDVI	0.55	<0.001	0.26	0.13	0.19	0.33
ENDVI	0.55	<0.001	0.87	<0.001	0.53	0.06
SAVI	0.79	<0.001	0.93	<0.001	0.00	0.98
NDVI	0.72	<0.001	0.83	<0.001	0.83	<0.001
NDRE	0.16	0.09	0.74	<0.001	0.71	0.02
RVI	0.74	<0.001	0.54	0.02	0.19	0.33
RECI	0.41	<0.001	0.48	0.03	0.00	1.00
EVI	0.68	<0.001	0.03	0.62	0.11	0.47
GNDVI	0.68	<0.001	0.44	0.04	0.67	0.02

RECI were significant for two of the varieties, while GDVI and EVI were significant only for one variety.

3.4. Relationship between sugarcane yield and normalized difference vegetation index

The Normalized Difference Vegetation Index (NDVI) values determined from canes of 4, 6, and 8 months of age and above were significantly ($P < 0.001$) correlated with the final yield of sugarcane in the N-14, NCo334 and B52298 varieties, respectively (Table 8). However, at 2, 4, and 6 months of age and below, the relationship between the NDVI and yields was not significant ($P < 0.05$), and the strength of the relationships were also very weak for the N-14, NCo334 and B52298 varieties, respectively (Table 8). The degree of association became stronger with an increase in cane age (Table 8), while it remained constant after eight months of age except for variety NCo334.

At harvest, variety NCo334 recorded the highest correlation with yield ($R^2 = 0.85$), followed by N14 ($R^2 = 0.81$) and B52298 ($R^2 = 0.73$), which is in agreement with the above results that all the field data of NCo334 are consistently well associated with LCVIs. At ten months of age, NCo334 and N14 showed equal degrees of association with yield ($R^2 = 0.81$), while both were greater than B52298 ($R^2 = 0.73$). In spite of the differences among the varieties, the observed relationship was reasonably strong and hence illustrates the capability of NDVI generated by Landviewer to indicate the performance of the cane and to use as a potential yield estimation tool. At eight months age of the cane, N-14 was found to be the highest in correlating with cane yield ($R^2 = 0.75$), preceding NCo334 ($R^2 = 0.58$) and B52298 ($R^2 = 0.34$). At the ages of 6, 4, and 2 months, N14 ($0.13 \leq R^2 \leq 0.69$) also showed the highest correlation with yield, followed by NCo334 ($0.04 \leq R^2 \leq 0.30$) and B52298 ($0.01 \leq R^2 \leq 0.12$), indicating that varieties considerably dictate the degree of relationship between sugarcane yield and NDVI.

4. Discussion

The main goal of this study was to evaluate the Landviewer Calculated Vegetation Indexes (LCVIs) and to identify the best VIs to be used in monitoring of sugarcane plantation. To this end, we evaluated the most commonly used vegetation indexes, which were calculated by the Landviewer platform by testing the goodness-of-fit of the sigmoid curve and evaluating its relationship with different growth parameters of sugarcane.

To our knowledge, this is the first study conducted in the country to test LCVIs in monitoring crops in general and sugarcane plantations in particular. Several studies in other countries verified that a significant and strong relationship existed between spectral vegetation indexes and ground truths such as biomass, yield, and leaf area index [68–71]. Hence, satellite remote sensing is useful to detect, map, and monitor the growth, health and productivity of crops [21]. However, the complexity of satellite image processing, which requires special facilities and skills, has restricted its wider application, particularly in Africa [26,29].

Despite the growing interest in satellite-based crop monitoring, only a few studies have been performed using the powerful and cloud-based satellite data processing platform called Landviewer [72,73]. The former study dealt with determining the state and dynamics of the ratio of vegetation and built-up area, while the latter focused on estimating water and vegetation area using Landviewer. Our results were similar to these previous studies in that LCVIs can effectively detect vegetation areas. Nevertheless, these studies had a limitation in that they did not test the accuracy and reliability level of different vegetation indexes calculated by the platform. In our study, we evaluated the effectiveness of ten LCVIs against ground truth data such as sigmoid growth pattern, yield components, FGCC, and yield of sugarcane, where we found promising results.

4.1. Goodness-of-fit of the sigmoid growth curve in LCVIs

The growth pattern of a plant often follows a sigmoidal curve where the rate of increase in growth is initially slow (lag phase), then becomes rapid (log/exponential phase) and ends with a steady rate (stationary phase) [74–76]. As such, sugarcane exhibits a similar growth pattern [16]. In our study, we confirmed that LCVIs significantly ($p < 0.001$) followed this type of pattern with different degrees of accuracy (Table 3). This confirms the reliability of using LCVIs for monitoring the performance of sugarcane crops and is useful for managing the problem of the continuous decline in cane yields in the country. Furthermore, the results suggest that studies pertaining to the growth patterns of a crop can use LCVIs.

Our findings are also compatible with those of Zhao et al. [77], who found that the NDVI readings increase rapidly as plants grow,

Table 8

Relationship between Normalized Difference Vegetation Index (NDVI) and yield of three sugarcane varieties at 2, 4, 8, 10 months of age and at harvest of the cane in Wonji-Shoa Sugarcane Plantation in central Ethiopia.

Time of NDVI Determination (Age in months)	NCo334		N-14		B52298	
	R ²	P-Value	R ²	P-Value	R ²	P-Value
2	0.04	0.27	0.126	0.06	0.01	0.65
4	0.03	0.43	0.519	<0.001	0.02	0.46
6	0.30	<0.001	0.69	<0.001	0.12	0.64
8	0.58	<0.001	0.75	<0.001	0.34	<0.001
10	0.81	<0.001	0.81	<0.001	0.73	<0.001
At harvest	0.85	<0.001	0.81	<0.001	0.73	<0.001

reaching near maximum levels about 200 days after planting for plant cane or 80–100 days after ratooning for ratoon crops. Ryu et al. [78] also conducted a similar study on rice using the conventional method of image processing. They found a sigmoid pattern in vegetation indexes (normalized difference vegetation index and photochemical reflectance index) fitted to cumulative growing degree-days of the plant with R^2 values of 0.94 and 0.83. Although we used days after planting/ratooning instead of degree days, our finding also showed comparable results.

The variations observed in the goodness of fit among the LCVIs (Table 3) imply that for robust sugarcane monitoring, growers should use specific VIs. In our study, we demonstrated that, with the exception of RECI and RVI, all LCVIs can be effectively utilized. The inferior performance observed in RECI and RVI (Table 3) may be attributed to the fact that both VIs are usually recommended to be used during the active growth stages of a crop or when a crop achieves good canopy cover and prior to the early phases of senescence, as they are designed to indicate crop chlorophyll content [45,79]. Hence, the lower vegetation tracking ability of these indexes during the early stages of sugarcane (when the vegetation is sparse) may have resulted in a lower goodness of fit compared to the other VIs.

The lower goodness of fit observed in ratoon crops may be attributed to the poor growth condition of this crop that emanates from the development of toxic chemicals in the rhizosphere, the low ability of ratoons to take up nutrients, the depletion of soil nutrients, soil compaction, and increased insect and disease incidence after harvest of plant cane crop [80]. As a result, the yield of ratoon cane is usually 10–30% less than that of plant cane crop [80,81].

4.2. Yield components of sugarcane

Cane density for all the three varieties, plant height for NCo334 and N14, and stalk diameter for NCo334 (except ENDVI) showed significant relationships with all the LCVIs (Table 4; Tables 5 and 6). The consistent performance of LCVIs in cane density agrees with the finding of Zhao et al. [82], who demonstrated that NDVI had a stronger relationship with cane density than with cane height and diameter. Zhao et al. [83] also demonstrated that among the five yield components they studied, stalk population along with yield exhibited the strongest associations with canopy reflectance. This may be related to the fact that plant density is the major determinant of canopy cover [84], which in turn influences VIs. It was also reported that sugarcane usually establishes a good crop stand whenever the plant density is higher [77,85]. Likewise, a plot with a high cane density may have a higher value of vegetation index than a plot with thicker and taller stalks that are fewer in number.

The differences observed among cane varieties were also noticed in the conventional method of satellite data processing. For instance, Lofton et al. [86] and Chanda et al. [87] corroborated that spectral reflectance can vary among varieties due to differences in canopy architecture. The three varieties considered in the current study varied considerably in their morphology [38], which could explain the observed differences. For instance, in variety N-14, the strength of the correlations between LCVIs and yield components were highest for plant height, which was in contrast to the other varieties where the strongest correlations were observed in plant density. This might be due to the unique growth feature of the N14 variety, which has a prostrate growth habit after germination, and canopies quickly turn erect with straight stalks. This variety is a fast sprouting type with a high tillering capacity, quick stalk growth rate, and canopy formation [88].

In variety B52298, the relationships between most of the LCVIs and the yield components (plant density, plant height, plant diameter) were weaker than those in the other varieties considered in our study. This might be attributed to the fact that variety B52298 is very sensitive to environmental stresses (drought, temperature, forest, etc.) so that the canopy appearance significantly varied during the growth period of the cane [89]. Therefore, monitoring this variety using LCVIs requires special precautions.

Generally, our study confirms the validity of LCVIs in assessing crop stands. Thus, there are possibilities of using LCVIs to generate information on the yield components of sugarcane, particularly plant density and height. As these parameters greatly determine the final yield of sugarcane [60,77,90], LCVIs can thus be employed to predict the cane yield. Furthermore, using LCVIs, it is possible to estimate various parameters of sugarcane, the costs of which are prohibitively high if done through conventional means. Supporting this postulation, Molijn et al. [16] reported that measuring various variables of sugarcane was very costly and prone to data errors due to the morphology and growing environment of the crop. Accordingly, all of the LCVIs can be effectively used to estimate cane population in all the three varieties, as well as cane height in NCo334 and N-14. However, in variety B52298, estimating plant height and diameter using LCVIs requires further study.

In this study, as the measurements of the different variables of yield components were conducted during the grand growth phase of sugarcane, further research needs to take into account different growth stages of the crop.

4.3. Fractional green canopy cover (FGCC)

Fractional green canopy cover (FGCC) is the percentage of the expected ground surface covered by photosynthetically active vegetation [64]. Thus, the significant relationship observed between FGCC and LCVIs (Table 7) again confirmed that LCVIs can effectively estimate the extent of greenness and ground coverage of sugarcane and thereby indicate the performance of the cane. However, there existed differences in the accuracy level of the vegetation indexes with varieties.

Studies conducted on the FGCC of sugarcane are very scant. We found only one study [91] that demonstrated the existence of significant relationships ($R^2 = 0.91$) between the germination rate of sugarcane and its FGCC, which was interpreted from digital photos analysed by Canopeo software. In the current study, we investigated the relationships between FGCC determined by the Canopeo software and spectral VIs (Table 7), where we found strong relationships. In a study conducted on other crops, NDVI was significantly correlated with FGCC [62–64,92], which is consistent with our findings. However, these studies have a limitation in that the researchers evaluated only NDVI.

Our study has demonstrated that NDVI, NDPI and GNDVI exhibited a consistent relationship with FGCC for all three varieties (Table 7). Earlier studies also indicated that these indexes are very dependable in indicating crop conditions. NDVI is sensitive to the presence of pigments that are involved in photosynthetic processes and is known to be efficient in delineating vegetation and detecting stress [93,94]. NDPI, on the other hand, is also acknowledged to have a high precision in both high- and low-biomass sites by replacing the red band with the “RED + SWIR”, thus removing the bare soil background effect [50,95] and minimizing vegetation index model saturation [96]. GNDVI has a larger dynamic range in dense vegetation and is more sensitive to chlorophyll concentration [52].

Even though ENDVI, SAVI, NDRE, RVI and RECI showed a significant relationship with FGCC in two of the varieties (NCo334 and N14), we observed an unexpected result in EVI (Table 7), where the relationship was significant only in one of the varieties. As corroborated in previous studies, EVI is one of the most effective indexes for vegetation cover assessment [70]. This may be the subject of further investigation.

4.4. Cane yield

Generation of the entire NDVI from planting to harvesting within a short time is one of the greatest advancements in remote-sensing technology that was realized by the Landviewer platform. This feature of the index saves a considerable amount of time during the evaluation of vegetation growth. In our study, we found that the time series NDVI generated by the platform was significantly correlated with cane yield at least starting from 6 months of cane age (Table 8). The coefficient of determinations (R^2) obtained in the current study (0.73–0.85) (Table 8) were comparable with similar studies conducted by the conventional method of image processing [27,67,97–100], where they found a coefficient determination ranging between 0.60 and 0.87. This again confirmed that the NDVI generated by the Landviewer platform is effective in indicating the ground truths.

Thus, our findings can be used as a basis to confidently utilize satellite-based crop monitoring in a sugarcane plantation by employing NDVI generated by the Landviewer platform. In view of the simplicity with which one can generate NDVI from the platform, it is a great opportunity for Ethiopian Sugarcane Plantations to fully exploit this technology so as to combat the decreasing trends of sugarcane yields. Through further investigation, Landviewer can also play a significant role in solving the problems pertaining to the conventional methods of yield estimation in sugarcane plantations, such as low accuracy, time constraints, and laboriousness.

In our study, the strongest correlations observed in the latter age of the cane (Table 8) were in line with De Almeida et al. [101] and Bégué et al. [67], who found that the maximum NDVI at 8–10 months of age and 2 months before harvest, respectively, had a significant correlation with sugarcane yield. Jaiphong et al. [102] also demonstrated that the final yield of sugarcane is determined at the grand growth phase (4–10 months), which is essential for actual cane formation, elongation, and yield build-up. Conversely, the weakest correlation during the early growth stages in this study might be attributed to the fact that the yield potential cannot be fully realized at the juvenile growth stage of sugarcane [86]. Furthermore, as Liu et al. [75] stated, the real field environment is complicated, with several elements that influence plant spectral properties. In particular, the possibility of weed interference in inflating the VIs might be high at the early growth stage of the cane, i.e., before canopy closure. On the other hand, the relatively poor correlation observed in variety B52298 might be related to its low resistance to various biotic and abiotic stresses [89]. This is also in agreement with the aforementioned results, where B52298 was poorly correlated, while NCo334 was strongly correlated with all the cane parameters considered in this study.

The findings of this study also imply the possibility of using Landviewer to monitor the performance of sugarcane starting from the juvenile growth stage. This is further depicted in Table 9 which is presented as example from one of the variety (NCo334) considered in this study. The table shows that out of the 29 sampled fields, the NDVI values of fields with the maximum and minimum yield levels showed drastic differences (16%–30%) at the different cane ages. Therefore, Landviewer can be employed as a tool to monitor sugarcane plantations and timely manage constraints that may have led to the continuous decline in yield. For instance, for the cane to give reasonably optimum yields, the NDVI values at different ages of the cane should be closer to the maximum NDVI listed below (Table 9). Otherwise, immediate investigations should be initiated to identify and solve the problem as early as possible.

The results clearly show that LCVIs are as effective as conventionally calculated indexes in correlating with the final yield of sugarcane. In addition, it is simple, user-friendly, and fast and can be managed by non-experts using ordinary computers or smartphones. This instils trust in the sugarcane plantation staff to utilize the Landviewer platform confidently. The utilization of the platform in turn improves the efficiency and effectiveness of plantation managers, which has enormous socioeconomic significance. This is because this technology can overcome the challenges of monitoring sugarcane plantations, which is difficult once the canopy is closed [16,17]. The technology also has the potential to minimize the expenses and efforts associated with estimating cane yield [21] which is one of the most important operation in a sugarcane plantation. Ultimately, satellite based crop monitoring by using LCVIs significantly contributes to managing the continuing decline in sugarcane yield, which costs WSSP around US\$ 8,228,558 per year [37]. However, it

Table 9

Normalized Difference Vegetation Index (NDVI) values of the sampled fields (variety NCo334) at different age of the cane with the maximum and minimum yields (ton ha^{-1}) of sugarcane at Wonji-Shoa Sugarcane Plantations in central Ethiopia.

Yield Level	Yield (ton ha^{-1})	NDVI at different ages (months) of the cane					
		2	4	6	8	10	Harvest
Maximum	134	0.476	0.706	0.721	0.761	0.788	0.788
Minimum	24.4	0.396	0.489	0.550	0.563	0.568	0.568
%Change	−82.1	−16.8	−30.7	−23.8	−26.0	−28.0	−28.0

is important to bear in mind that anomalies in data owing to cloud cover and weed interference are the major challenges of satellite-based crop monitoring. In fact, the advancements being made in satellites equipped with hyperspectral and active sensors are expected to play a pivotal role in minimizing the effects of these challenges.

Generally, our study has several strengths, such as considering up to ten vegetation indexes, six parameters, three major varieties, and two crop types. Furthermore, we used the actual cane yield so that the validity of the results would be reasonable. However, our findings have the following limitations. First, we focused only on three dominant varieties. From current and previous studies [86], it is evident that varietal differences matter, and thus, it is worth subjecting every commercial variety to this platform. Second, the study was conducted on one sugarcane plantation (WSSP, central Ethiopia), and the effect of location should be further studied. Third, the capability of LCVIs to identify the type of stresses such as moisture, nitrogen, salinity stress, etc., should be investigated. Fourth, the study employed only the Sentinel-2A satellite, which is one of the eleven satellites in the platform. Finally, to make use of the multiple features of the platform, further evaluation should be continued.

5. Conclusions

The results of our study demonstrated that a sigmoid growth curve was significantly fitted to the Landviewer Calculated Vegetation Indexes (LCVIs) profile of sugarcane. The yield components, fractional green canopy cover, and final yield of sugarcane also had significant associations with LCVIs. Therefore, LCVIs and the time series NDVI generated by the platform can be used effectively to monitor sugarcane plantations. Furthermore, three of the vegetation indexes, i.e., the Normalized Difference Phenology Index (NDPI), Normalized Differential Vegetation Index (NDVI) and Soil Adjusted Vegetation Index (SAVI), were identified as the most effective indexes and should be preferentially employed during crop monitoring. In light of the difficulty in conventional methods of satellite image processing, the promising performance observed in LCVIs creates an excellent opportunity for developing countries to exploit the potential of satellite technology. Particularly, this has paramount importance for Ethiopian Sugarcane Plantations for identifying and mitigating production constraints that have led to a continuously drastic decline in cane yields. Furthermore, remote sensing research can make use of LCVIs. Beyond crop monitoring, Landviewer has several features, such as the detection of moisture, nutrients, salinity, pests, etc., that need further evaluation.

Author contribution statement

Alemayehu Dengia: Conceived and designed the experiments; Performed the experiments; Analysed and interpreted the data; Wrote the paper.

Nigussae Dechassa: Analysed and interpreted the data; Contributed reagents, materials, Analysis tools or data; wrote the paper.

Lemma Wogi and Berhanu Amsalu: Analysed and interpreted the data; Contributed reagents, materials, Analysis tools or data.

Data availability statement

Data will be made available on request.

Additional information

The Landviewer platform is available at the following open source <https://eos.com/products/landviewer>.

Declaration of competing interest

The authors declare that they have no known competing financial interests or personal relationships that could have appeared to influence the work reported in this paper.

Acknowledgements

The authors thank the Ethiopian Sugar Industry Group for funding the research. Thanks are also due to Wonji-Shoa Sugar Factory and Wonji Research Station for providing the yield data and collecting field data for the research. EOS-Data Analytics deserves special gratitude for developing and providing such a simplified and user-friendly platform free of charge.

References

- [1] P.H. Moore, F.C. Botha, *Sugarcane: Physiology, Biochemistry, and Functional Biology*, John Wiley & Sons, Inc, New Delhi, India, 2014.
- [2] S. Afghan, M.E. Khan, W.R. Arshad, K.B. Malik, A. Nikpay, Economic importance and yield potential of sugarcane in Pakistan, in: B.K. Ghimire (Ed.), *Sugarcane - its Products and Sustainability*, IntechOpen eBooks, 2023, <https://doi.org/10.5772/intechopen.105517>.
- [3] F.L. Ambetsa, S.C. Mwangi, S.N. Ndirangu, Technical efficiency and its determinants in sugarcane production among smallholder sugarcane farmers in Malava sub-county, Kenya, *Afr. J. Agric. Res.* 15 (3) (2020) 351–360.
- [4] Z. Thibane, S. Soni, L. Phali, L. Mdoda, Factors impacting sugarcane production by small-scale farmers in KwaZulu-Natal Province-South Africa, *Heliyon* 9 (1) (2023), e13061, <https://doi.org/10.1016/j.heliyon.2023.e13061>.
- [5] S.R. Travella, D. Oliveira, *Sugarcane in Africa*. www.vib.be/en/about-biotech-news/Documents/vib_fact_sugarcane_EN_2017_1006_LR_single.pdf.

- [6] A. Kassie, African Labour and foreign capital: the case of wonji-shewa sugar estate in Ethiopia, 1951-1974, *Soc. Sci.* 11 (5) (2022) 245–253, <https://doi.org/10.11648/j.ss.20221105.11>.
- [7] R. Fauconnier, *Sugarcane, the Tropical Agriculturalist*, Macmillan press ltd, London, 1993.
- [8] R.S. Verma, *Sugarcane Production Technology in India*, Lacknow, International book distributing co, 2004.
- [9] S. Van Berkum, P. Roza, F. Van Tongeren. Impacts of the EU sugar policy reforms on developing countries, 2005. No. 1075-2016-87045.
- [10] R. Ming, P.H. Moore, K. Wu, A. D'Hont, J.C. Glaszmann, T.L. Tew, Sugarcane improvement through breeding and biotechnology, in: J. Janick (Ed.), *Plant Breeding Reviews*, umc 27, John Wiley & Sons, Inc, 2006, pp. 15–126.
- [11] N. Abraham, A. Girum, N. Tadesse, T. Bineyam, A. Abiy, A. Fikru, *Sugar Technology Roadmap (Addis Ababa, Ethiopia)*, in: Ministry of Science and Technology, vol. 1, 2017.
- [12] T. Alemayehu, S. Bastiaanssen, K. Bremer, Y. Cherinet, S. Chevalking, M. Girma, *Water Productivity Analyses Using WaPOR Database. A Case Study of Wonji, Ethiopia*. Water-PIP Technical Report Series, IHE Delft Institute for Water Education, Delft, the Netherlands, 2020.
- [13] M.O. Dinka, J.M. Ndambuki, Identifying the potential causes of waterlogging in irrigated agriculture: the case of the wonji-shoa sugar cane plantation (Ethiopia), *Irrigat. Drain.* 63 (1) (2014) 80–92, <https://doi.org/10.1002/ird.1791>.
- [14] D. Alemayehu, E. Lantinga, Impact of long-term conventional cropping practices on some soil quality indicators at Ethiopian Wonji Sugarcane Plantation, *Advances in Crop Sciences and Technology* 4 (2016) 224. <https://doi.org/10.4172/2329-8863.1000224>.
- [15] W. Tesfaye, Status of selected physicochemical properties of soils under long term sugarcane cultivation fields at Wonji-Shoa Sugar Estate, *Am. J. Agric. For.* 9 (2021) 397–408, <https://doi.org/10.11648/j.ajaf.20210906.19>.
- [16] R.A. Molijn, L. Iannini, J.V. Rocha, R.F. Hanssen, Ground reference data for sugarcane biomass estimation in São Paulo state, Brazil, *Sci. Data* 5 (2018), 180150, <https://doi.org/10.1038/sdata.2018.150>.
- [17] S.P. Singh, A. Kumar, H.L. Kushwaha, Sugar cane canopy spraying: a perspective solution with ergonomics and mechatronics approach, *Sugar Technology* 22 (2020) 203–207, <https://doi.org/10.1007/s12355-019-00766-1>.
- [18] ILO, *Hazardous Child Labour in Agriculture: Sugarcane*. International Programme on the Elimination of Child Labour Safety and Health, Fact sheet: International Labour Office, Geneva, 2004.
- [19] B. Li, Y. Ling, M. Tian, S. Zheng, Design and implementation of sugarcane growth monitoring system based on RFID and ZigBee, *International Journal of Online Engineering* 14 (3) (2018) 96, <https://doi.org/10.3991/ijoe.v14i03.8413>.
- [20] F.C. de Oliveira Maia, V.B. Bufon, V.B. Bufon, T.P. Leão, Vegetation indices as a tool for mapping sugarcane management zones, *Precis. Agric.* 24 (1) (2022) 213–234, <https://doi.org/10.1007/s11119-022-09939-7>.
- [21] J. Som-ard, C. Atzberger, E. Izquierdo-Verdiguier, F. Vuolo, M. Immitzer, Remote sensing applications in sugarcane cultivation: a review, *Rem. Sens.* 13 (20) (2021) 4040, <https://doi.org/10.3390/rs13204040>.
- [22] S. Khanal, K. Kc, J.P. Fulton, S. Shearer, E. Ozkan, Remote sensing in agriculture—accomplishments, limitations, and opportunities, *Rem. Sens.* 12 (22) (2020) 3783, <https://doi.org/10.3390/rs12223783>.
- [23] M. Polivova, A. Brook, Detailed investigation of spectral vegetation indices for fine field-scale phenotyping, in: E.C. Carmona, A.C. Ortiz, R.Q. Canas, C. M. Musarella (Eds.), *Vegetation Index and Dynamics*, IntechOpen, 2021, <https://doi.org/10.5772/intechopen.96882>.
- [24] A. Bhargava, Climate change, demographic pressures and global sustainability, *Econ. Hum. Biol.* 33 (2019) 149–154, <https://doi.org/10.1016/j.ehb.2019.02.007>.
- [25] K. Jindo, O. Kozan, K. Iseki, B. Maestrini, F.K. van Evert, W. Yilma, E. Arai, Y.E. Shimabukuro, Y. Sawada, C. Kempenaar, Potential utilization of satellite remote sensing for field-based agricultural studies, *Chemical and Biological Technologies in Agriculture* 58 (2021) 8, <https://doi.org/10.1186/s40538-021-00253-4.25>.
- [26] C. Nakalembe, I. Becker-Reshef, R. Bonifacio, G. Hu, M.L. Humber, C.J. Justice, J. Keniston, K. Mwangi, K. Rembold, S. Shukla, F. Urbano, A.K. Whitcraft, Y. Li, Zappacosta, M. Ian Jarvis, A. Sanchez, A review of satellite-based global agricultural monitoring systems available for Africa, *Global Food Secur.* 29 (2021), 100543, <https://doi.org/10.1016/j.gfs.2021.100543>.
- [27] G. Abebe, T. Tadesse, B. Gessesse, Combined use of Landsat 8 and Sentinel 2A imagery for improved sugarcane yield estimation in Wonji-Shoa, Ethiopia, *Journal of the Indian Society of Remote Sensing* 50 (1) (2022) 143–157, <https://doi.org/10.1007/s12524-21-01466-8>.
- [28] Z. Zhang, M. Liu, X. Liu, G. Zhou, A new vegetation index based on multitemporal Sentinel-2 images for discriminating heavy metal stress levels in rice, *Sensors* 18 (7) (2018) 2172.
- [29] S. Fritz, L. See, J.C.L. Bayas, F. Waldner, D. Jacques, I. Becker-Reshef, A. Whitcraft, B. Baruth, R. Bonifacio, J. Crutchfield, F. Rembold, O. Rojas, A. Schucknecht, M. Van der Velde, J. Verdin, B. Wu, N. Yan, L. You, S. Gilliams, S. Mùcher, R. Tetrault, I. Moorthy, I. McCallum, A comparison of global agricultural monitoring systems and current gaps, *Agric. Syst.* 168 (2019) 258–272, <https://doi.org/10.1016/j.agsy.2018.05.010>.
- [30] L.N. Zhichkina, V.V. Nosov, K.A. Zhichkin, H.T. Aydinov, V.N. Zhenzhebir, V.V. Kudryavtsev, Satellite monitoring systems in forestry, *J. Phys.* 1515 (2020), 032043.
- [31] P. Kolodiy, M. Pidlypna, The improvement of the agricultural yields forecasting model using the software product “Landviewer”, *Geomatics and Environmental Engineering* 14 (1) (2020) 59–67, <https://doi.org/10.7494/geom.2020.14.1.59>.
- [32] B. Wakjira, Assessment of client satisfaction on family planning services utilization in wonji hospital, Ethiopia, *JBR Journal of Clinical Diagnosis and Research* 5 (1) (2017), <https://doi.org/10.4172/2376-0311.1000137>.
- [33] M. Bona, N. Deyessa, A.M. Begosew, M. Azage, Occupational health and safety practices and associated factors among workers in Ethiopia’s Metehara and Wonji sugar industries: a convergent parallel mixed design, *BMJ Open* 13 (2) (2023), e065382, <https://doi.org/10.1136/bmjopen-2022-065382>.
- [34] FAO, *World Reference Base for Soil Resources*, ISBN 92-5-104141-5, FAO, ISRIC and ISSS, 1998, <https://www.fao.org/3/w8594e/w8594e00.htm>.
- [35] D. Ruffeis, W. Loiskandl, R. Spendlingwimmer, M. Schonercklee, S.B. Awulachew, E. Boelee, K. Wallner, Environmental impact analysis of two large scale irrigation schemes in Ethiopia pp. 370-388, in: Awulachew, S.B; Loulseged, M.; Yilma, A.D. (Comps.). *Impact of Irrigation on Poverty and Environment in Ethiopia: Draft Proceedings of the Symposium and Exhibition*, Addis Ababa, Ethiopia, 27-29 November 2007. Colombo, Sri Lanka: International Water Management Institute (IWMI), 2007, <https://doi.org/10.22004/ag.econ.246407>.
- [36] A. Jones, H. Breuning-Madsen, M. Brossard, A. Dampha, J. Deckers, O. Dewitte, T. Gallali, S. Hallett, R. Jones, M. Kilasara, P. Le Roux, E. Michéli, L. Montanarella, O. Spaargaren, L. Thiombiano, E. Van Ranst, M. Yemefack, R. Zougmore, *Soil Atlas of Africa*, European Commission, Publications Office of the European Union, 2013, <https://doi.org/10.2788/52319>.
- [37] D. Alemayehu, D. Nigussae, W. Lemma, A. Berhanu, Analysis of declining trends in sugarcane yield at wonji-shoa sugar estate, Central Ethiopia, *Experimental Results* 4 (2023) e13, <https://doi.org/10.1017/exp.2023.13>.
- [38] A.L. Khan, K.A. Tadesse, B.L. Robe, A study on morphological characters of introduced sugarcane varieties (saccharum spp., hybrid) in Ethiopia, *Int. J. Plant Breed. Genet.* 11 (1) (2017) 1–12, <https://doi.org/10.3923/ijpb.2017.1.12>.
- [39] N. Djamaï, R. Fernandes, Comparison of SNAP-derived sentinel-2A L2A product to ESA product over europe, *Rem. Sens.* 10 (6) (2018) 926, <https://doi.org/10.3390/rs10060926>.
- [40] F. Chen, C. Ming, J. Li, C. Wang, M. Claverie, A comparison of sentinel-2a and sentinel-2b with preliminary results, *Environmental Science* (2018), 211249302. Corpus ID.
- [41] J. Li, B. Chen, Optimal solar zenith angle definition for combined landsat-8 and sentinel-2A/2B data angular normalization using machine learning methods, *Rem. Sens.* 13 (13) (2021) 2598, <https://doi.org/10.3390/rs13132598>.
- [42] D. Xu, C. Wang, J. Chen, M. Shen, B. Shen, R. Yan, Z. Li, A. Karnieli, J. Chen, Y. Yan, X. Wang, The superiority of the normalized difference phenology index (NDPI) for estimating grassland aboveground fresh biomass, *Rem. Sens. Environ.* 264 (2021), 112578, <https://doi.org/10.1016/j.rse.2021.112578>.
- [43] A. Huete, K. Didan, T. Miura, L.G. Ferreira, Overview of the radiometric and biophysical performance of the MODIS vegetation indices, *Rem. Sens. Environ.* 83 (2002) 195–213, [https://doi.org/10.1016/S0034-4257\(02\)00096-2](https://doi.org/10.1016/S0034-4257(02)00096-2).

- [44] T.M. Susantoro, K. Wikantika, A. Saepuloh, A.H. Harsolumakso, Selection of Vegetation Indices for Mapping the Sugarcane Condition Around the Oil and Gas Field of North West Java Basin, Indonesia, IOP Conference Series: Earth and Environmental Science, Volume 149, the 4th International Symposium on LAPAN-IPB Satellite for Food Security and Environmental Monitoring 9–11 October, Bogor, Indonesia, 2017.
- [45] EOS crop monitoring guide. <https://eos.com/products/crop-monitoring/user-guide/>. (Accessed 12 May 2022).
- [46] C.J. Strong, N.G. Burnside, D. Llewellyn, The potential of small-Unmanned Aircraft Systems for the rapid detection of threatened unimproved grassland communities using an Enhanced Normalized Difference Vegetation Index, *PLoS One* 12 (10) (2017), e0186193, <https://doi.org/10.1371/journal.pone.0186193>.
- [47] R.P. Sripada, R.W. Heiniger, J.G. White, A.D. Meijer, Aerial color infrared photography for determining early in-season nitrogen requirements in corn, *Agronomy* 9 (2017) 968–977, <https://doi.org/10.2134/agronj2015.0200>.
- [48] J.W. Rouse Jr., R.H. Haas, D.W. Deering, J.A. Schell, J.C. Harlan, Monitoring the Vernal Advancement and Retrogradation (Green Wave Effect) of Natural Vegetation (No. E75-10354), 1974.
- [49] A. Huete, A soil-adjusted vegetation index (SAVI), *Rem. Sens. Environ.* 25 (3) (1988) 295–309, [https://doi.org/10.1016/0034-4257\(88\)90106-x](https://doi.org/10.1016/0034-4257(88)90106-x).
- [50] C. Wang, J. Chen, J. Wu, Y. Tang, P. Shi, A.T. Andrew Black, K. Zhu, A snow-free vegetation index for improved monitoring of vegetation spring green-up date in deciduous ecosystems, *Rem. Sens. Environ.* 196 (2017) 1–12, <https://doi.org/10.1016/j.rse.2017.04.031>.
- [51] G. Ritchie, C. Bednarz, Estimating defoliation of two distinct cotton types using reflectance data, *J. Cotton Sci.* 9 (2005) 182–188.
- [52] A.A. Gitelson, Y.J. Kaufman, M.N. Merzlyak, Use of a green channel in remote sensing of global vegetation from EOS-MODIS, *Rem. Sens. Environ.* 58 (1996) 289–298, [https://doi.org/10.1016/S0034-4257\(96\)00072-7](https://doi.org/10.1016/S0034-4257(96)00072-7).
- [53] R.L. Pearson, L.D. Miller, Remote mapping of standing crop biomass for estimation of the productivity of the short-grass Prairie, in: *8th International Symposium on Remote Sensing of Environment*, Pawnee National Grassland, Colorado, 1972, pp. 1357–1381.
- [54] Y. Tan, J.Y. Sun, B. Zhang, M. Chen, Y. Liu, X.D. Liu, Sensitivity of a ratio vegetation index derived from hyperspectral remote sensing to the brown plant hopper stress on rice plants, *Sensors* 19 (2) (2019) 375, <https://doi.org/10.3390/s19020375>.
- [55] A. Michael, S-shaped growth curve. A dictionary of ecology. *Encyclopedia.com*. (Accessed 7 June 2022). <https://www.encyclopedia.com>.
- [56] Liying Cao, P. Shi, L. Li, G. Chen, A new flexible sigmoidal growth model, *Symmetry* 11 (2) (2019) 204, <https://doi.org/10.3390/sym11020204>.
- [57] S.A. Jane, F.A. Fernandes, E.M. Silva, J.A. Muniz, T.J. Fernandes, G.V. Pimentel, Adjusting the growth curve of sugarcane varieties using nonlinear models, *Ciência Rural*. 50 (3) (2020) 1–10, <https://doi.org/10.1590/0103-8478cr2019040857>.
- [58] P. Verhulst, La loi d'accroissement de la population, *Nouv. Mem. Acad. R. Soc. Belle-Lettre. Bruxelles*. 18 (1845) 1.
- [59] B. Gompertz, On the nature of the function expressive of the law of human mortality, and on a new mode of determining the value of life contingencies, *Philosophical Transactions of the Royal Society* 115 (1825) 513–583, <https://doi.org/10.1098/rspl.1815.0271>.
- [60] E. Tena, F. Tadesse, F. Million, D. Tesfaye, Phenotypic diversity, heritability, and association of characters in sugarcane genotypes at Metehara Sugar Estate, Ethiopia, *J. Crop Improv.* (2022) 1–24, <https://doi.org/10.1080/15427528.2022.2158979>.
- [61] A. Patrignani, T.E. Ochsner, Canopeo: a powerful new tool for measuring fractional green canopy cover, *Agron. J.* 107 (2015) 2312–2320, <https://doi.org/10.2134/agronj15.0150>.
- [62] J.M. Jáuregui, F.G. Delbino, M.I.B. Bonvini, G. Berhongaray, Determining yield of forage crops using the Canopeo mobile phone app, *Journal of New Zealand Grasslands* (2019) 41–46, <https://doi.org/10.33584/jnzg.2019.81.385>.
- [63] R. Heinonen, T.J. Mattila, Smartphone-based estimation of green cover depends on the camera used, *Agron. J.* 13 (6) (2021) 5597–5601, <https://doi.org/10.1002/agj2.20752>.
- [64] T.R. Tenreiro, M. García-Vila, J.A. Gómez, J.A. Jiménez-Berni, E. Fereres, Using NDVI for the assessment of canopy cover in agricultural crops within modelling research, *Comput. Electron. Agric.* 182 (2021), 106038, <https://doi.org/10.1016/j.compag.2021.106038>.
- [65] *Vsn International, Genstat for Windows 18th Edition*. VSN International, Web page: Genstat.co.uk, Hemel Hempstead, UK, 2015.
- [66] C. Zaiontz, *Real Statistics Using Excel*, 2020. www.real-statistics.com.
- [67] A. Bégue, V. Lebourgeois, E. Bappel, P. Todoroff, A. Pellegrino, F. Baillarin, B. Siegmund, Spatio-temporal variability of sugarcane fields and recommendations for yield forecast using NDVI, *Int. J. Rem. Sens.* 31 (20) (2010) 5391–5407, <https://doi.org/10.1080/01431160903349057>.
- [68] S. Das, T.P. Singh, Correlation analysis between biomass and spectral vegetation indices of forest ecosystem, *Int. J. Eng. Res. Technol.* 1 (5) (2012) 1–13. ISSN: 2278-0181.
- [69] A.B. Alfaca, B. Sílio, S.B. Pereira, R. Filgueiras, F.F. Cunha, Sugarcane spatial-temporal monitoring and crop coefficient estimation through NDVI, *Rev. Bras. Eng. Agrícola Ambient.* 23 (5) (2019) 330–335, <https://doi.org/10.1590/1807-1929/agriambi>.
- [70] N. Mzid, F. Cantore, G. Mastro, R. Albrizio, M.H. Sellami, M. Todorovic, The application of ground-based and satellite remote sensing for estimation of biophysiological parameters of wheat grown under different water regimes, *Water* 12 (2020) 2095, <https://doi.org/10.3390/w12082095>.
- [71] M. Maitiniazvi, V. Sagan, P. Sidike, A.M. Daloye, H. Erkbol, F.B. Fritschi, Crop monitoring using satellite/UAV data fusion and machine learning, *Rem. Sens.* 12 (9) (2020) 1357, <https://doi.org/10.3390/rs12091357>.
- [72] V. Yukhnovskiy, O. Zibteva, Green space trends in small towns of Kyiv region according to EOS Land Viewer—a case study, *J. For. Sci.* 66 (6) (2020) 252–263.
- [73] K. Das, Application of modern geospatial tools in vegetation and water estimation; a case study in Burisuti Pather Wetland Area of Assam, in: R. Sarkar (Ed.), *Environmental Sustainability in the 21st Century: Emerging Issues and the Way Forward*, Namya Press, Delhi, 2020, pp. 221–232.
- [74] X. Yin, J. Goudriaan, E.A. Lantinga, J. Vos, H.J. Spiertz, A Flexible sigmoid function of determinate growth, *Ann. Bot. (Lond.)* 91 (2003) 361–371.
- [75] J.H. Liu, Y. Yan, A. Ali, M. Yu, Q. Xu, P. Shi, L. Chen, Simulation of crop growth, time to maturity and yield by an improved sigmoidal model, *Sci. Rep.* 8 (2018) 7030, <https://doi.org/10.1038/s41598-018-24705-4>.
- [76] J. Khonghintaiong, P. Songsri, N. Jongrungraklang, Understanding growth rate patterns among different drought resistant sugarcane cultivars during plant and ratoon crops encountered water deficit at early growth stage under natural field conditions, *Agronomy* 11 (10) (2021) 2083, <https://doi.org/10.3390/agronomy11102083>.
- [77] D. Zhao, M. Irey, C. LaBorde, C. Hu, Identifying physiological and yield-related traits in sugarcane and energy cane, *Agron. J.* 109 (3) (2017) 927–937, <https://doi.org/10.2134/agronj2016.10.0585>.
- [78] J.H. Ryu, H. Jeong, Cho, J. Performances of vegetation indices on paddy rice at elevated air temperature, heat stress, and herbicide damage, *Rem. Sens.* 12 (16) (2020) 2654, <https://doi.org/10.3390/rs12162654>.
- [79] R.D. Jackson, A.R. Huete, Interpreting vegetation indices, *Prev. Vet. Med.* 11 (3–4) (1991) 185–200.
- [80] DAWN, Increasing yield of ratoon sugarcane. <https://www.dawn.com/news/296976/increasing-yieldof-ratoon-sugarcane>. (Accessed 7 June 2023) (Scribe Publishing Platform).
- [81] P.D. Riajaya, B. Hariyono, M. Cholid, F.T. Kadarwati, B. Santos, D. Busro, S. Subiyakto, Growth and yield potential of new sugarcane varieties during plant and first ratoon crops, *Sustainability* 14 (21) (2022), 14396, <https://doi.org/10.3390/su142114396>.
- [82] D. Zhao, M. Irey, C. LaBorde, C.J. Hu, Physiological and yield characteristics of 18 sugarcane genotypes grown on a sand soil, *Crop Sci.* 59 (6) (2019) 2741–2751, <https://doi.org/10.2135/cropsci2019.02.0107>.
- [83] D. Zhao, V.S. Gordon, J.C. Comstock, N.C. Glynn, R.M. Johnson, Assessment of sugarcane yield potential across large numbers of genotypes using canopy reflectance measurements, *Crop Sci.* 56 (4) (2016) 1747–1759, <https://doi.org/10.2135/cropsci2015.12.0747>.
- [84] J. Xu, J. Ma, Y. Tang, W. Wu, J. Shao, W. Wu, S. Wei, Y. Liu, Y. Wang, H. Guo, Estimation of sugarcane yield using a machine learning approach based on UAV-LiDAR data, *Rem. Sens.* 12 (17) (2020) 2823, <https://doi.org/10.3390/rs12172823>.
- [85] S. Matsuoka, R. Stolf, Sugarcane tillering and ratooning: key factors for a profitable cropping, *Sugarcane: Production, cultivation and uses* 5 (2) (2012) 137–157.
- [86] J. Lofton, B.S. Tubana, Y. Kanke, J. Teboh, H. Viator, M. Dalen, Estimating sugarcane yield potential using an in-season determination of normalized difference vegetative index, *Sensors* 12 (6) (2012) 7529–7547, <https://doi.org/10.3390/s120607529>.

- [87] S. Chanda, Y. Kanke, M. Dalen, J. Hoy, B. Tubana, Coefficient of variation from vegetation index for sugarcane population and stalk evaluation, *Agrosystems, Geosciences & Environment* 1 (1) (2018) 1–9. <https://doi.org/10.2134/age2018.07.0016>.
- [88] A. Wondimu, H. Legesse, T. Fite, Effects of time gap between seed cane cutting to the planting of sugarcane varieties on growth parameter and yield of sugarcane (*saccharum* spp. hybrid) at finca'a sugar estate, Ethiopia, *Sugar Tech* 24 (2) (2021) 485–493, <https://doi.org/10.1007/s12355-021-01035-w>.
- [89] D. Alemayehu, K. Demlash, Influence of durations between seedcane cutting and planting on sprouting of sugarcane at Wonji Sugar Estate, *Proceeding of Ethiopian Sugar Industry Biannual Conference 2* (2013) 200–207.
- [90] M.I. Masri, A.B.A. El-Taib, F.F.B. Abu-El-lail, Genetic and phenotypic correlation and path coefficient analysis for traits in sugarcane, *SVU-International Journal of Agricultural Sciences 4* (2) (2022) 53–64.
- [91] M. Alimohammadi, E. Panahpour, A. Nseri, Evaluation of the effect of nano-nitrogen chelate fertilizer on germination and green cover of sugarcane seedlings by digital images, *Iranian Journal of Soil Research* 32 (4) (2019) 483–493, <https://doi.org/10.22092/ijsr.2019.118557>.
- [92] P. Lykhovoyd, R. Vozhegova, S.O. Lavrenko, N.M. Lavrenko, The study on the relationship between normalized difference vegetation index and fractional green canopy cover in five selected crops, *Sci. World J.* (2022) 1–6, <https://doi.org/10.1155/2022/8479424>.
- [93] A.R. Formaggio, I.D.A. Sanches, *Sensoriamento remoto em agricultura, Oficina de Textos* 288p (2017).
- [94] S. Huang, L. Tang, J.P. Hupy, Y. Wang, G. Shao, A commentary review on the use of normalized difference vegetation index (NDVI) in the era of popular remote sensing, *J. For. Res.* 32 (1) (2021) 1–6, <https://doi.org/10.1007/s11676-020-01155-1>.
- [95] X. Chen, Z. Guo, J. Chen, W. Yang, Y. Yao, Y. Zhang, X. Cui, X. Cao, Replacing the red band with the red-SWIR band ($0.74_{\text{pred}} + 0.26_{\text{pswir}}$) can reduce the sensitivity of vegetation indices to soil background, *Rem. Sens.* 11 (7) (2019) 851, <https://doi.org/10.3390/RS1107085>.
- [96] N. Djamai, F. Richard, W. Marie, M. Heather, G. Kalifa, Validation of the sentinel simplified level 2 product prototype processor (SL2P) for mapping cropland biophysical variables using Sentinel-2/MSI and Landsat-8/OLI data, *Rem. Sens. Environ.* 225 (2019) 416–430, <https://doi.org/10.1016/j.rse.2019.03.020>.
- [97] J. Morel, P. Todoroff, A. Bégué, A. Bury, J. Martiné, M. Petit, Toward a satellite-based system of sugarcane yield estimation and forecasting in smallholder farming conditions: a case study on reunion island, *Rem. Sens.* 6 (7) (2014) 6620–6635, <https://doi.org/10.3390/rs6076620>.
- [98] S.K. Dubey, A.S. Gavli, S.K. Yadav, S. Sehgal, S.S. Ray, Remote sensing-based yield forecasting for sugarcane (*Saccharum officinarum* L.) crop in India, *Journal of the Indian Society of Remote Sensing* 46 (11) (2018) 1823–1833, <https://doi.org/10.1007/s12524-018-0839-2>.
- [99] M.M. Rahman, A. Robson, Integrating Landsat-8 and Sentinel-2 time series data for yield prediction of sugarcane crops at the block level, *Rem. Sens.* 12 (8) (2020) 1313, <https://doi.org/10.3390/rs12081313>.
- [100] K. Krupavathi, M. Raghubabu, A. Mani, P.R.K. Parasad, L. Edukondalu, Field-scale estimation and comparison of the sugarcane yield from remote sensing data: a machine learning approach, *Journal of the Indian Society of Remote Sensing* 50 (2) (2022) 299–312, <https://doi.org/10.1007/s12524-021-01448-w>.
- [101] T.I.R. De Almeida, C.R. De Souza Filho, R. Rossetto, ASTER and Landsat ETM+ images applied to sugarcane yield forecast, *Int. J. Rem. Sens.* 27 (19) (2006) 4057–4069, <https://doi.org/10.1080/01431160600857451>.
- [102] T. Jaiphong, J. Tominaga, K. Watanabe, R. Suwa, M. Ueno, Y. Kawamitsu, Changes in photosynthesis, growth, and sugar content of commercial sugarcane cultivars and *Erianthus* under flood conditions, *Plant Prod. Sci.* 20 (1) (2017) 126–135, <https://doi.org/10.1080/1343943X.2016.1275711>.